

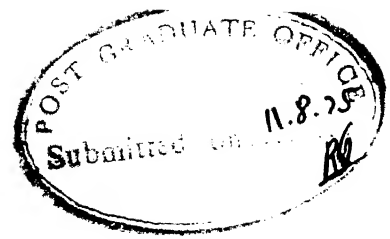
# COMPUTER SIMULATION OF SCATTERING FUNCTIONS FOR THE KANPUR-NAINITAL RAKE TROPOSCATTER SYSTEM

A Thesis Submitted  
in partial Fulfilment of the Requirements  
for the Degree of  
MASTER OF TECHNOLOGY

By  
CAPT. C. T. RAMA RAO

to the

DEPARTMENT OF ELECTRICAL ENGINEERING  
INDIAN INSTITUTE OF TECHNOLOGY KANPUR  
AUGUST, 1975



### CERTIFICATE

Certified that this work 'A Computer Simulation of Scattering Functions for the Kanpur - Nainital Rake Tropo-scatter System' by Capt. C.T. Rama Rao has been carried out under my supervision and that this has not been submitted elsewhere for a degree.

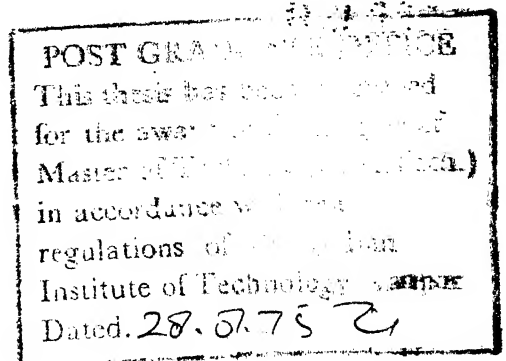
*N.C. Mathur*

Dr. N.C. MATHUR

Professor

Department of Electrical Engineering  
Indian Institute of Technology  
KANPUR.

8 August, 1975



Shelley  
621.28195  
R18



ILLINOIS PUR  
CENTRAL LIBRARY  
Acc. No. A 45558

TH  
EC/1975 M  
R18C

1 FEB 1976

## TABLE OF CONTENTS

	<u>Page No.</u>
ACKNOWLEDGEMENTS	i
ABSTRACT	ii
CHAPTER 1 INTRODUCTION	1
1.1 Brief Historical Background of Rake Concept Measurements of Scattering Function	1
1.2 Details of the Problem	3
1.3 Out line of Work	4
CHAPTER 2 KANPUR - NAINITAL TROPOSCATTER LINK DETAILS	6
2.1 Link Parameters	6
2.2 Common Volume Geometry	6
2.3 Antenna Gain Pattern	9
2.4 Modulation Signal	10
CHAPTER 3 BRIEF DISCUSSION ON RAKE SYSTEM MEASU- REMENTS	12
3.1 Basic Rake Measurement Concept	12
3.2 Tap Unit Spacing Consideration	15
3.3 Rake System for Kanpur - Nainital Troposcatter Link	16
CHAPTER 4 SIMULATION MODEL OF THE TROPOSPHERE	24
4.1 Doppler Shift Tropospheric Scatter Model	24
4.2 Antenna Gain Pattern and Antenna Off Set Effects	29



	4.3 Angular Dependence Function	30
	4.4 Ambiguity Function	34
	4.5 Magnitude Weighting Function	35
	4.6 Delay Shell - Scattering Volume	35
	4.7 Discussion	38
CHAPTER 5	SCATTERING FUNCTIONS; DELAY - DOPPLER POWER SPECTRA	40
	5.1 Delay Doppler Locus for a Single Layer	40
	5.2 Simulation of Scattering Functions	43
	5.2.1 Scattering Functions:Set-1	43
	5.2.2 Scattering Functions:Set-2	48
	5.2.3 Scattering Functions:Set-3	52
	5.2.4 Scattering Functions:Set-4	57
	5.2.5 Scattering Functions:Set-5	61
	5.2.6 Scattering Functions:Set-6	65
	5.2.7 Scattering Functions:Set-7	70
CHAPTER 6	REFRACTIVE INDEX STRUCTURE FUNCTION COEFFICIENT $C_n^2$	77
	6.1 Refractive Index Structure Funct- ion Coefficient $C_n^2$	77
	6.2 Evaluation of $C_n^2$ from Rake Data	78
CHAPTER 7	CONCLUSION	86
	7.1 Applications of the Simulated Scattering Functions	86
	7.2 Suggestions	89

	<u>Page No.</u>
APPENDICES	
A-1	Program for Computing and Plotting of Delay Shells 90
A-2	Program for Computing and Plotting of Scattering Functions 93
A-3	Program for Computing the Relative Zero- Doppler Power of the Rake Receiver Correlators 97
REFERENCES	100

## ACKNOWLEDGEMENTS

I am extremely grateful to Prof. N.C. Mathur for his continuous guidance, supervision and encouragement throughout this work. Sincere thanks are due to Dr. T.R. Vishwanathan for providing IBM 1800 plotter facility.

I finally thank Mr. C.M. Abraham for his excellent typing.

Kanpur,  
7 August, 1975.

C. T. Rama Rao  
Capt. C.T. RAMA RAO

## ABSTRACT

The Rake troposcatter technique as a tool for channel sounding has been studied in this report with reference to the Kanpur - Nainital troposcatter link. The technique consists of transmitting a pseudo random (PN) sequence of pulses over a troposcatter channel. At the receiver, the received signal is correlated with identical replicas of the PN sequence, generated locally, with different delays introduced to account for the multipath delays. Such a technique yields delay - doppler plots termed scattering functions which characterise the channel.

Digital computer programs are developed through this study to simulate the results of Rake troposcatter technique based on a certain model for scattering. The output of a single correlator, called a tap yields a doppler spectrum which depends upon a number of factors. Scattering volume available within the midpath plane region common to a scattering layer and a chosen time delay shell serves as a first estimate of the shape and location of the doppler spectrum. Antenna gain patterns, antenna offsets, angular dependence functions and Rake modulation signal ambiguity functions are employed as modifiers or weighting functions

of the first estimate to obtain a final estimate of the doppler spectrum for the choosen delay.

The scattering functions for various beam swinging experiments, for different, scattering layer heights, scattering layer thickness and for multiple layers having different degree of anisotropy are simulated. The relative zero doppler power received at each Rake tap, which gives the relative measure of retractive index structure function coefficient  $C_n^2$ , is evaluated.

The resulting scattering functions indicate the role of various factors such as heights of scattering layers and their thicknesses, wind velocity, anisotropy of scattering turbulence, wave-number dependence of the spectrum of turbulence, etc., on the receiver output. It is shown that these parameters can be studied with the help of a Rake system.

## CHAPTER 1

### INTRODUCTION

#### Background

#### 1.1 Brief Historical/of Rake Concept and Measurements of Scattering Function

The Rake concept of measurement involves transmission of a special wide - bandwidth signal through the tropospheric scatter channel to a correlation type of radio receiver. The signal, in its passage through the scatter channel, encounters a dynamic multipath situation that rather uniquely disperses (or spreads) the signal in both time delay and frequency. The receiver output signals can be employed through further computer processing for obtaining delay doppler power spectrums or scattering functions. The scattering function graphically display the doppler spectrum of the signal received with different delays.

The Rake concept was first introduced by Price and Green [1] in 1958 for the purpose of solving the multipath problems associated with high frequency digital data communications via the ionosphere. Only in more recent years has the concept been applied to measurement of tropospheric scatter propagation characteristics by

Barrow [2] and Birkemeier [3]. Barrow [2] carried out the experiments over two paths - a 480 kms overland path and a 614 kms over water path. The aim of his experiments was to record the randomly varying in phase and quadrature components of each Rake tap output and thus investigate the fluctuations in signal phase, as well as in amplitude caused by fading. Scattering functions were obtained, which clearly illustrate the distribution of received signal energy as a function of multipath time delay and doppler frequency shift. Birkemeier [3] carried out experiments for remote sensing of the lower atmospheric refractive structure. The detected atmospheric structures showed spatial refractive inhomogeneity in the form of discrete scattering layers at different heights. Birkemeier [4] in 1973 carried out Rake soundings over a pathlength of 270 kms and the results have been compared with meteorological soundings of the refractive index structure determined from radiosonde ascents near the common volume. It was observed by him that the received signal zero - doppler power profile indicated more power than was predicted by refractive index structure function coefficient  $C_n^2$ .

## 1.2 Details of the Problem

A troposcatter link has been set-up between Kanpur and Nainital and a Rake system hardware is being developed for this link. The data obtained from the Rake system can be usefully employed to study some tropospheric characteristics. In this report some theoretical calculations are carried out to indicate the type of output expected from the Rake system under various meteorological conditions.

A computer program has been developed to plot scattering functions, for the parameters of the experimental Kanpur - Nainital troposcatter link using a Rake system. Scattering functions are simulated for the following common volume characteristics and experimental set-ups :

- (a) Single scattering layer in the common volume
- (b) Multiple scattering layers in the common volume
- (c) Antenna azimuthal and elevation off sets
- (d) Different values of power index 'p' of power spectrum of refractivity fluctuations.

The relative zero doppler power received at each Rake tap, which gives the relative measure of



Refractive Index Structure Function coefficient  $C_n^2$ , is evaluated.

### 1.3 Outline of Work

This work has been divided into various Chapters. In Chapter 2 link details, common volume geometry and the modulation signal to be used have been given in brief. In Chapter 3, basic Rake measurement concept is given in detail, so that one can visualize how the concept is applied in the development of simulation program. Experimental Rake System for Kanpur - Nainital troposcatter link is also discussed in this chapter. In Chapter 4 tropospheric scattering model as described by Birkemeier[3] is given in conjunction with other areas that effect the received signal characteristics such as antenna off set effects, angular dependence, ambiguity function and magnitude weighting function. In Chapter 5 a digital computer simulation program is developed based upon the Rake concept of measurements as developed (in Chapter 3) and the tropospheric scattering model as given (in Chapter 4). Then scattering functions for various common volume characteristics and the beam swinging experiments are simulated and plotted. Chapter 6 treats

the refractive index structure function coefficient  $C_n^2$  and its evaluation by the zero doppler power profiles. Chapter 7 deals with several applications of the digital computer simulation of scattering Functions and concludes this report.

Simulation program has been written in Fortran IV language and IBM-1800 is used for this work. Scattering Functions and constant delay shells have been drawn by IBM-1627 plotter.

## CHAPTER 2

## KANPUR - NAINITAL TROPOSCATTER LINK DETAILS

2.1 Link Parameters

The Kanpur - Nainital troposcatter link has been described by Gupta [5] and its geometry is shown in Fig. 2.1. The frequency of operation of the link is 2.1 GHz (a wavelength of 14.286 cms). Transmitter and receiver antennas are situated at a height of 4.3 Mtrs and 18.4 Mtrs above ground level (1892.3 Mtrs and 145.8 Mtrs AMSL respectively) at Nainital and Kanpur respectively. The effective radius of earth is taken as 8500 KMS. Total distance (2D) between transmitter and receiver is 330 KMS.

2.2 Common Volume Geometry

Calculations in respect of common volume geometry have been done by Gupta [5] and the same are used for simulation. The following are the common volume parameters which are used in this work :

- (a) Grazing ray height ( $Z_G$ ) = 1.8 KMS.
- (b) Scattering angle ( $\theta$ ) = 38.8 MR.
- (c) Length of the common volume = 141 KMS.

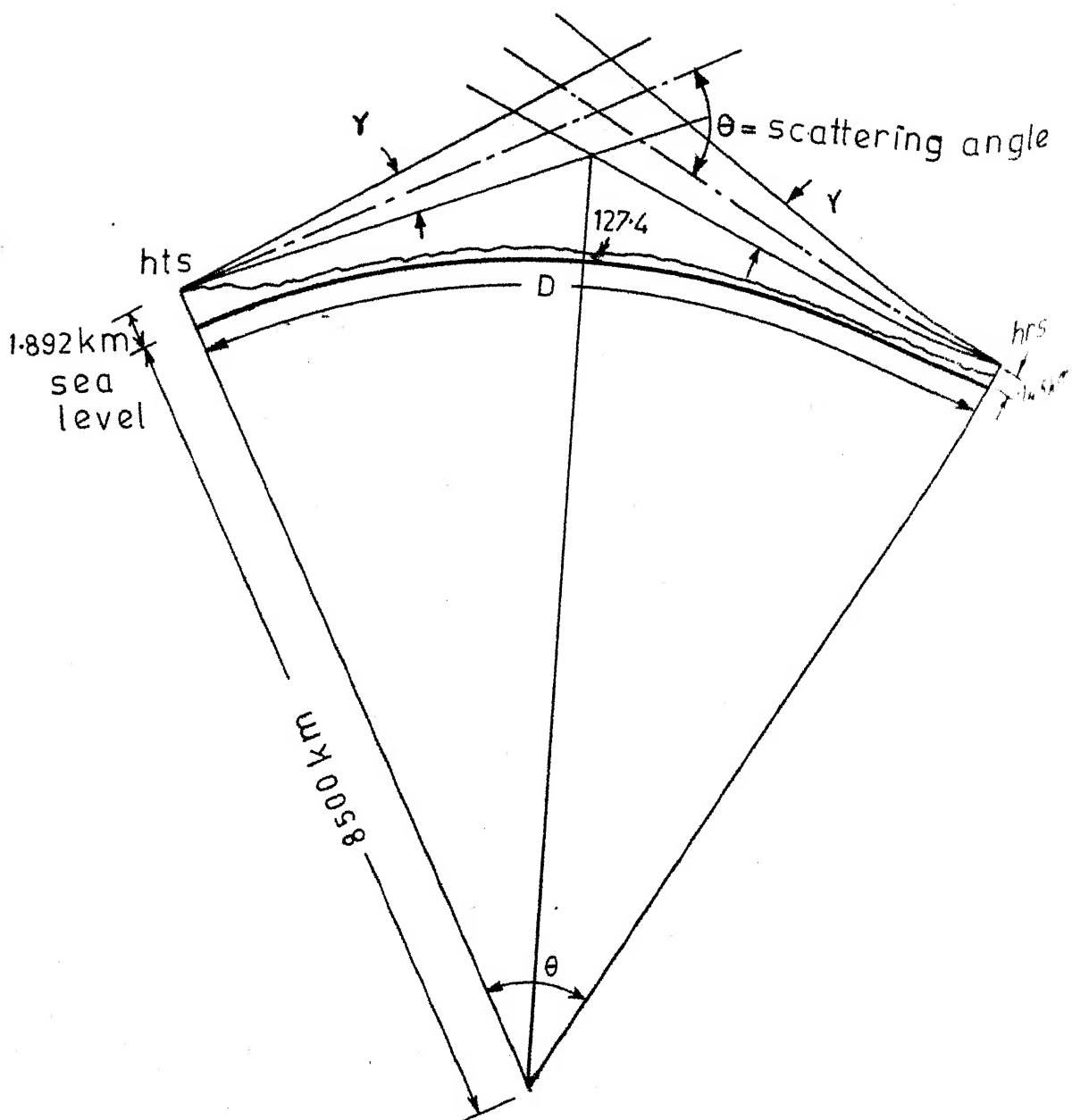


FIG. 2-1 LINK GEOMETRY



- (d) Height of the centre of the common  
volume above earth's surface = 3.2 KMS
- (e) Diagonal width of the common  
volume = 2.8 KMS.

Common volume geometry for this tropo link is shown in Fig. 2.2.

### 2.3 Antenna Gain Pattern

The product of transmitter and receiver antenna gain is referred to as combined antenna gain and can be expressed as

$$G = G_T (X,Y,Z) G_R (X,Y,Z) \quad (2.1)$$

Throughout the simulation work in this report Gaussian circular antenna gain pattern is assumed. The combined antenna gain in Y-direction by using Gaussians can be expressed as

$$G = \text{Exp} \left[ - (Y - Y_c)^2 / Y_n^2 \right] \quad (2.2)$$

where,

Y = Cross path distance in KMS from the centre of the beam

$Y_c$  = Beam off set distance in KMS at the mid path

$Y_n^2$  = Variance (2.6 KMS<sup>2</sup> for the antenna used on Kanpur - Nainital troposcatter link).

The radius of the circle of the antenna pattern at the mid path is calculated as 3 kms for a 3 db beam width of 0.96 degrees.

#### 2.4 Modulation Signal

Very short periodic pulses spaced sufficiently apart so that the multipath response die out between successive pulses, can be used for channel sounding. The disadvantage is high peak to average power ratio. In a Rake system this is overcome by using a constant amplitude signal - a radio frequency carrier that is pseudo-randomly modulated in phase by a PN sequence obtained from a PN sequence generator. PN sequences are chosen because (i) their auto correlation function has a central peak of value equal to length of sequence and the side-lobe is of unit height, (ii) the cross correlation of a PN sequence and its shifted version is zero.

On the Kanpur - Nainital troposcatter link, at the transmitter, a PN sequence of length  $(2^{15} - 1)$  i.e., 32, 767 bits is used to phase modulate the carrier at 10 M bauds. So the transmitted PN sequence period (T) is 3.2767 milli secs. At the receiver, the received signal is split into in phase and quadrature components which are cross correlated with identical binary streams

derived from PN sequence generators, each of which is delayed successively by 0.1 micro secs. This provides a multipath delay resolution ( $\tau$ ) of 0.1 micro secs. However, a multipath delay resolution of 0.05 micro-secs is used for simulation in this work.



## CHAPTER 3

## BRIEF DISCUSSION ON RAKE SYSTEM MEASUREMENTS

3.1 Basic Rake Measurement Concept

Rake as a communication system is designed to work against the combination of random multipath and additive noise disturbances. This has been proposed by Price and Green [1]. In channel sounding experiments, using Rake principle, the interest is to get a continuous record of quadrature components of channel impulse response  $\beta(\tau, t)$  as suggested by POOL [6]. From this data, it is possible to observe multipath structure, doppler shifts and calculate the scattering function which adequately characterise the tropo-channel.

As an over-the-horizon propagation medium, the troposphere is assumed to have the form of a linear time varying filter. So the input - output relationships of the tropospheric channel may be specified by the equivalent low pass impulse response  $\beta(\tau, t)$  which is output response of the channel, measured at time  $t$ , due to a unit impulse input applied at time  $(t, \tau)$ . The term 'Rake' applies to a class of measurement methods wherein a transmitted signal is modulated in a manner that allows

Signal

the received signal modulation to be cross-correlated with delayed replicas of the transmitted signal modulation to provide estimates of  $\beta(\tau, t)$  at several specific time delay values,  $\tau_k$ , where  $k = 1, 2, \dots, N$ .

Let  $u_0(t)$ , be a series of unit impulses equally spaced in time at intervals of  $T$ , starting at a time  $t_0$ ,

$$\text{i.e. } u_0(t) = \sum_n \delta[t - (t_0 + nT)] \quad (3.1)$$

$$n = 0, 1, 2, \dots$$

If  $u(t)$  be the received signal, then  $u(t)$  is given by

$$u(t) = \int_{-\infty}^{\infty} \beta(\tau, t) u_0(t - \tau) d\tau \quad (3.2)$$

which is the convolution of the channel input with the impulse response of the channel. Substituting (3.1) in (3.2) and interchanging the order of summation and integration,  $u(t)$  is given by

$$u(t) = \sum_n \left\{ \int_{-\infty}^{\infty} \beta(\tau, t) \delta[t - (t_0 + nT) - \tau] d\tau \right\} \quad (3.3)$$

Using the shifting property of the unit impulses

$$u(t) = \sum_n \beta[t - (t_0 + nT); t] \quad (3.4)$$

From (3.4) it is observed that the received signal is a series of impulse responses resulting from unit impulses applied at time  $(t_0 + nT)$ .

To calculate scattering functions, it is essential to measure  $\beta(\tau, t)$  at fixed values of delay, i.e. measurements of  $\beta(\tau_K, t)$ .  $\beta(\tau_K, t)$  can be obtained by cross-correlating the received signal with a delayed replicas of the transmitted signal, as given by

$$R_{uu}(\tau_K) = \frac{1}{I} \int_I u(t) u_0^*(t - \tau_K) dt \quad (3.5)$$

Substituting (3.1) and (3.4) in (3.5).

$$R_{uu}(\tau_K) = \frac{1}{I} \int_I \sum_m \beta[t - (t_0 + mT); t] \sum_n \delta[t - (t_0 + nT) - \tau_K] dt \quad (3.6)$$

The value of (3.6) is zero, except when  $m = n$ . Interchanging the order of summation and integration,

$$R_{uu}(\tau_K) = \frac{1}{I} \sum_n \int_I \beta(t - (t_0 + nT); t] \delta[t - (t_0 + nT) - \tau_K] dt \quad (3.7)$$

where  $I$  = integration interval =  $T$ .

$$R_{uu}(\tau_K) = \frac{1}{T} \sum_n \beta[\tau_K, t_0 + nT + \tau_K] = \frac{1}{T} \beta(\tau_K, t) \quad (3.8)$$

The measurement process involved in obtaining the equation (3.8) forms the basis of the Rake concept which is illustrated in Fig. 3.1.

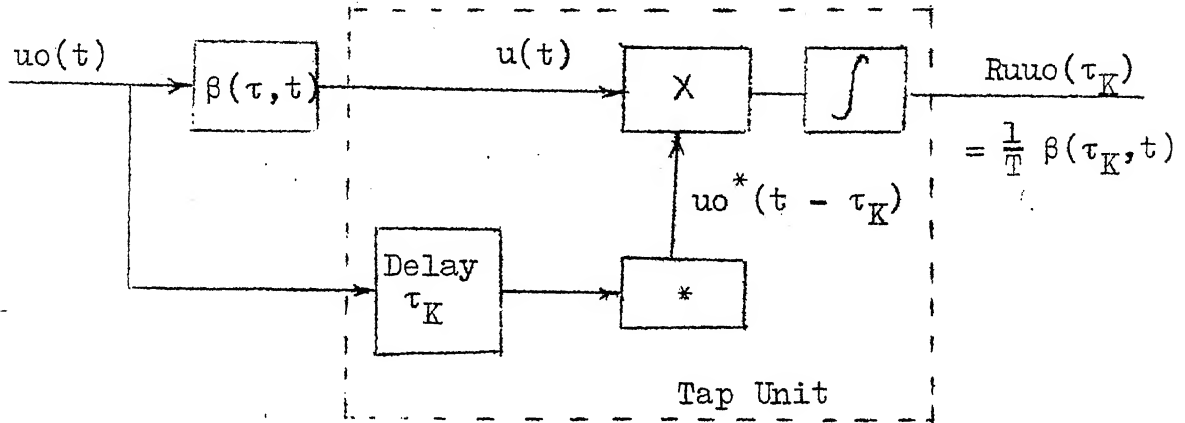


Figure 3.1

The structure of  $\beta(\tau, t)$  can be estimated by paralleling a sufficient number of tap units, each having a different reference delay. Consecutive tap unit outputs form a series of unit impulses representing the auto correlation of the transmitted modulation signal at specific values of  $\tau$ . A plot of such a series of unit impulse auto-correlations resembles the teeth of garden rake in appearance, providing a basis for the term 'Rake'.

### 3.2 Tap Unit Spacing Considerations

Minimum tap unit spacing is a function of the time resolution capabilities of the transmitted modulation,

or probing signal. Maximum time, or delay resolution obtainable with a given probing signal is an inverse function of the effective bandwidth of the signal.

$$\text{i.e., Tap unit spacing} = \frac{1}{\text{Effective bandwidth}}$$

If, Tap unit spacing =  $\tau$ , and effective bandwidth is WHz, then,

$$\tau = \frac{1}{W} \quad (3.9)$$

For the experimental set up of Kanpur - Nainital troposcatter link a Rake system is being built with multipath resolution of 0.1 micro-secs. For the simulation work, however, a delay resolution of 0.05 micro secs is used. There are 19 Rake taps, delays from 0.05  $\mu$ sec to 0.95  $\mu$ sec with increments of 0.05  $\mu$ sec.

### 3.3 Rake System for Kanpur - Nainital Troposcatter Link

The transmitter in a Rake system consists of the following sub-systems :

- (a) a highly stable oscillator from which other desired frequencies are synthesised
- (b) PN sequence generator

- (c) phase modulator ; and
- (d) band pass filter

The receiver consists of :

- (a) highly stable oscillator (synchronised with the transmitter oscillator) and frequency synthesiser
- (b) Mixer
- (c) IF Amplifier
- (d) Demodulator
- (e) PN sequence generator
- (f) Two correlators at each Rake tap one for estimating inphase and the other for quadrature component of  $\beta(\tau, t)$ .

At the receiver the received signal is demodulated to get the inphase and quadrature components. This can be achieved by using the arrangement given in Fig. 3.2.

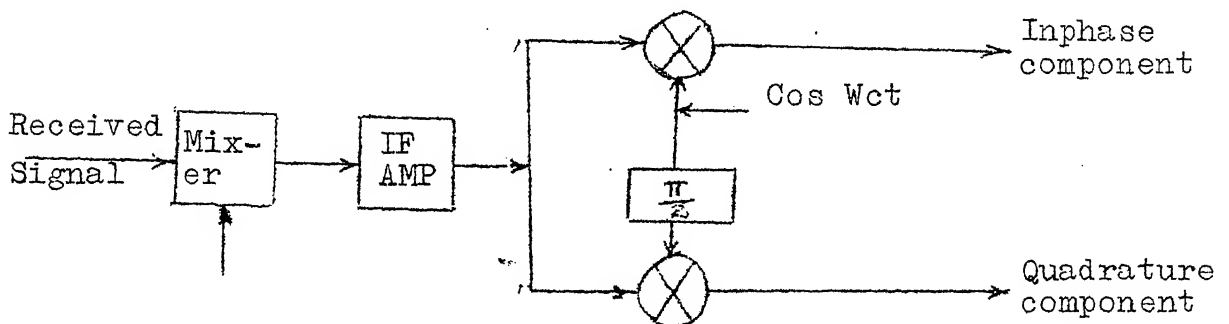


Fig. 3.2

For the experimental set up on Kanpur - Nainital troposcatter link two Rake systems are considered based on the Rake systems built at University of Wisconsin (Rake I, Birkemeier 1969) and at Sylvania (Rake II, Barrow 1965). The transmitter is same for both <sup>Rake I and</sup> ~~Rake II~~ as shown in Fig. 3.3.

Rake System I employs analog signal processing with attendant requirements on gain and frequency stabilities and is expected to have large dynamic range. Rake System II, on the other hand, is less complex in hardware and is an all digital system. The synchronisation between transmitter and receiver is achieved by using 5 MHz Rubidium clock from which all other desired frequencies are synthesised. 15 Bit shift register generates the PN sequence which is transmitted at 10 mega baud rate after phase modulation. The final carrier frequency is 2100 MHz.

At the receiver of Rake I, Fig. 3.4, the received signal is heterodyned with 2160 MHz to get IF of 60 MHz, which is then resolved into inphase and quadrature components by product demodulation. These are then correlated with the  $\tau$  shifted version of the reference PN sequence at 15 Rake taps having two correlators at

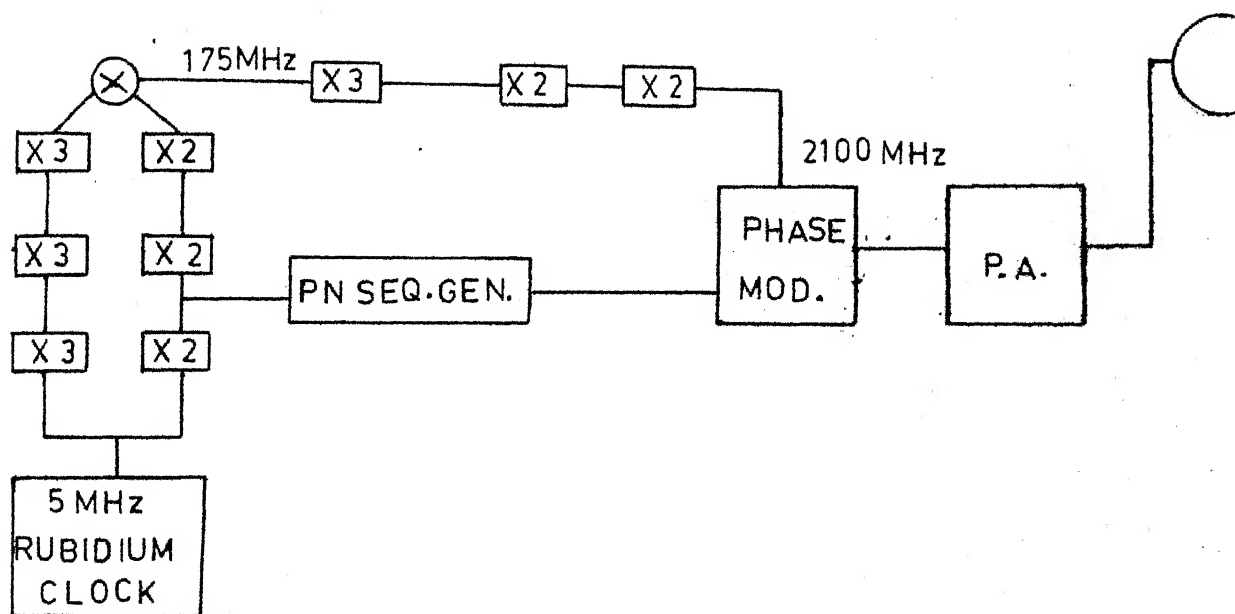


FIG.3-3 TRANSMITTER



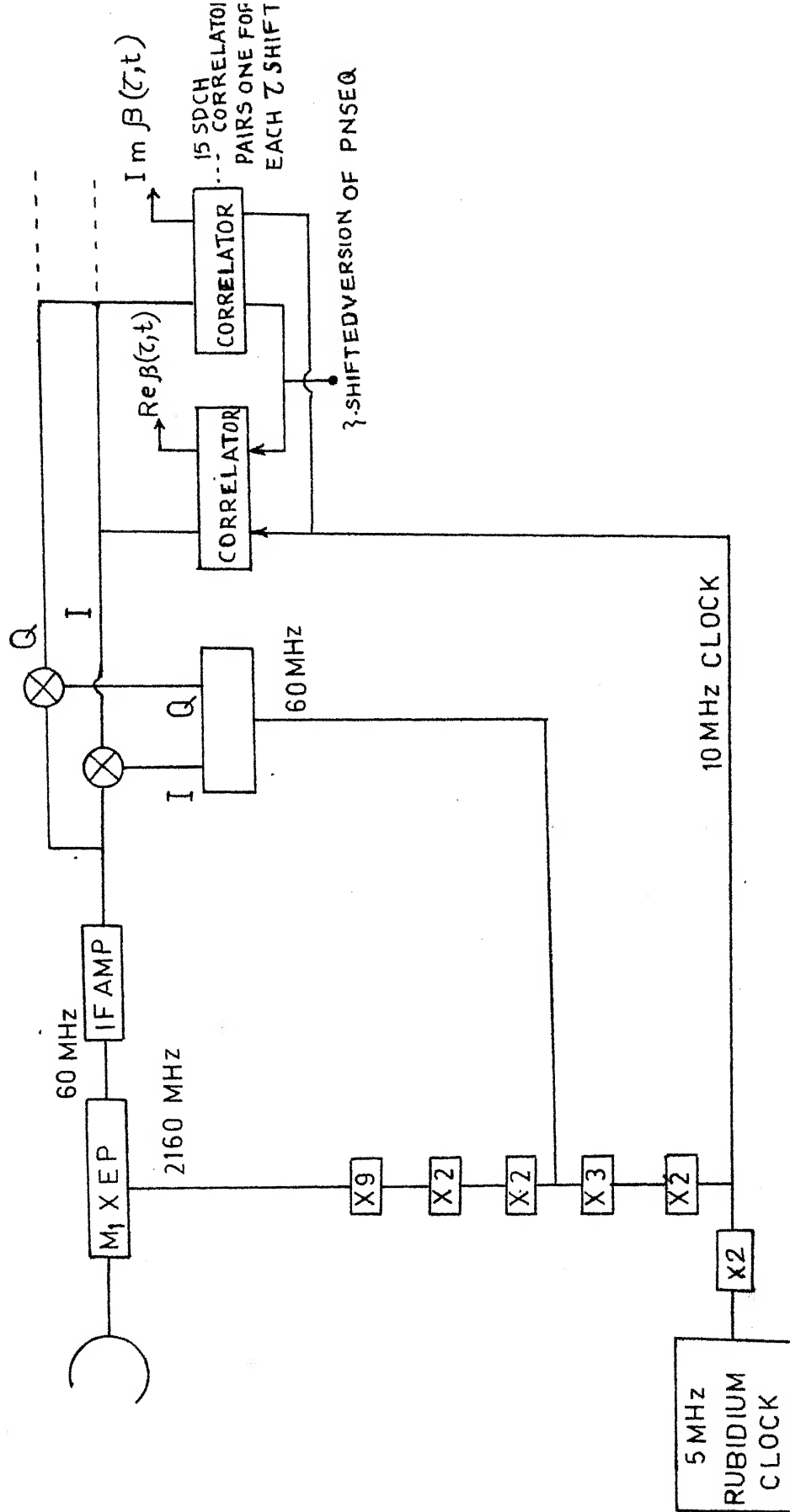


FIG. 3-4 RECEIVER FOR RAKE I

each tap one for inphase and one for quadrature component. The correlation is achieved by using current switch which is the heart of the system. In this system the signal processing is done throughout in the analog mode. The expected dynamic range is 80 db.

At the receiver of Rake II, Fig. 3.5, after demodulation the quadrature and inphase components of the signal are obtained in binary form. The components are then cross correlated with the  $\tau$  shifted version PN sequence by bit by bit modulo-2 addition and counting at the 15 Rake taps. Barrow has shown that the counter output gives minimum error estimate of  $\beta(\tau, t)$  under low SNR conditions of the received signal. Hence Gaussian noise is added deliberately at the IF stage. The dynamic range of this Rake System is about 20 db.

The overall system characteristics are given as under :

- |                            |  |
|----------------------------|--|
| (a) Operating frequency    | - 2.1 GHz  |
| (b) Transmission Technique | - AM   |
| (c) IF Frequency           | - 60 MHz   |
| (d) Sounding signal        | - PN sequence of<br>period $(2^{15} - 1)$<br>bits corresponding<br>to 3.2767 milliseecs. |

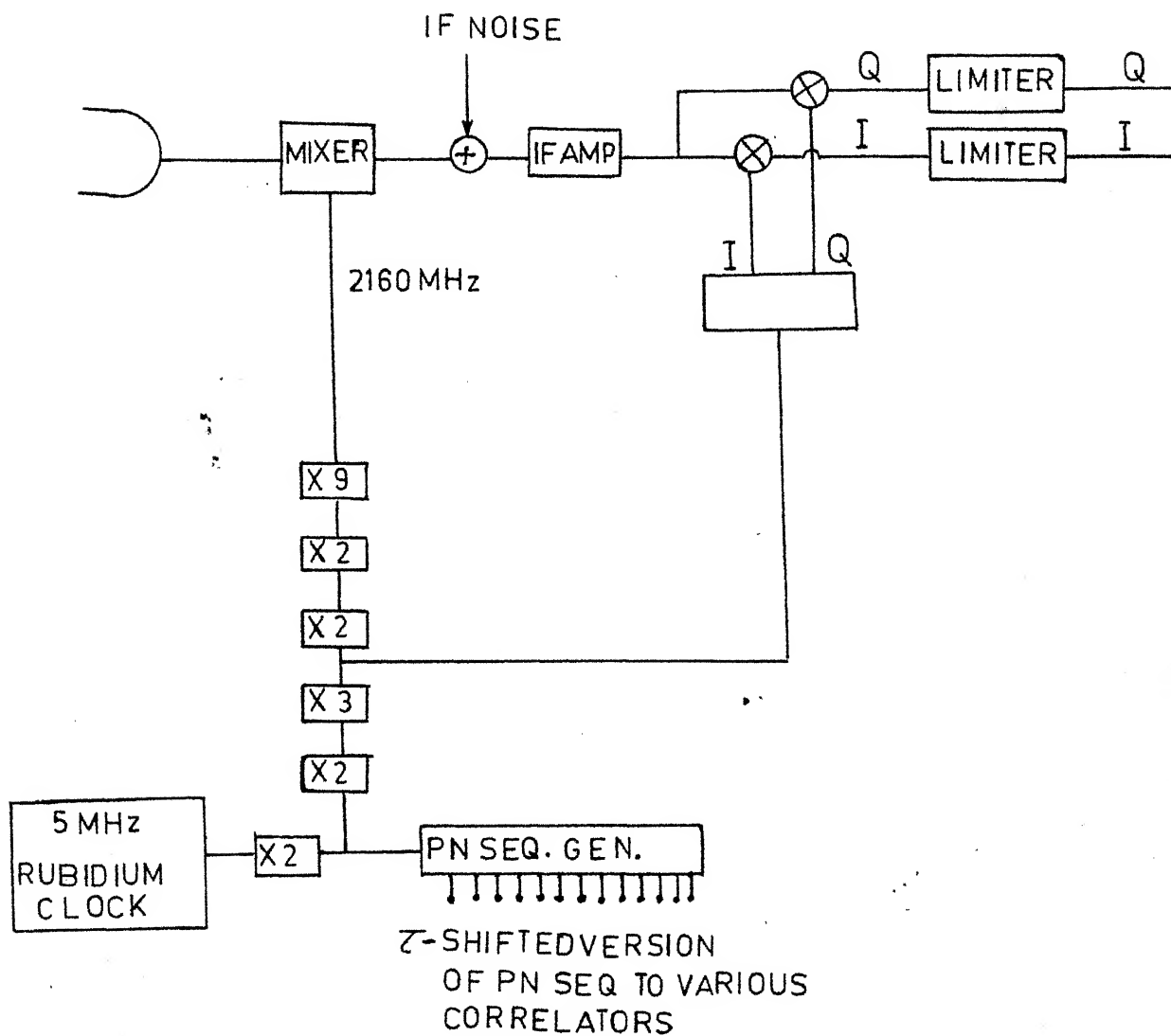


FIG.3-5 RECEIVER FOR RAKE II

- (e) Method of signal modulation - PS keying at  
10 M bauds
- (f) Signal bandwidth - 10 MHz
- (g) Multipath resolution - 0.1 microsecs.
- (h) Mode of propagation - Overland scatter
- (i) Link range - 330 KMS

## CHAPTER 4

## SIMULATION MODEL OF THE TROPOSPHERE

4.1 Doppler Shift Tropospheric Scatter Model

A doppler shift model suggested by Birkemeier [3] is considered in this work. Birkemeier has suggested that the scattering mechanism can be described as consisting of a large number of discrete scatterers confined to one or more relatively thin horizontal layers wherein the scatterers drift along with the wind. Such a discrete scatterer hypothesis lends itself to the digital computation of the total received scatter signal, at a given instant of time, as the sum of the signal voltages received via each individual scatterer present in the antenna pattern common volume region.

The doppler shift model shown in Fig. 4.1 locates the transmitter, receiver and scatterers in an X,Y,Z co-ordinate system with the origin at the mid point of the chord line of length 2D that joins the transmitter and receiver. Assuming multiple scattering effects are negligible, then the ray path length L (X,Y,Z) is defined as the distance from the transmitter through the scatterer to the receiver.

$$L(X,Y,Z) = [(D+X)^2 + Y^2 + Z^2]^{\frac{1}{2}} + [(D-X)^2 + Y^2 + Z^2]^{\frac{1}{2}} \quad (4.1)$$

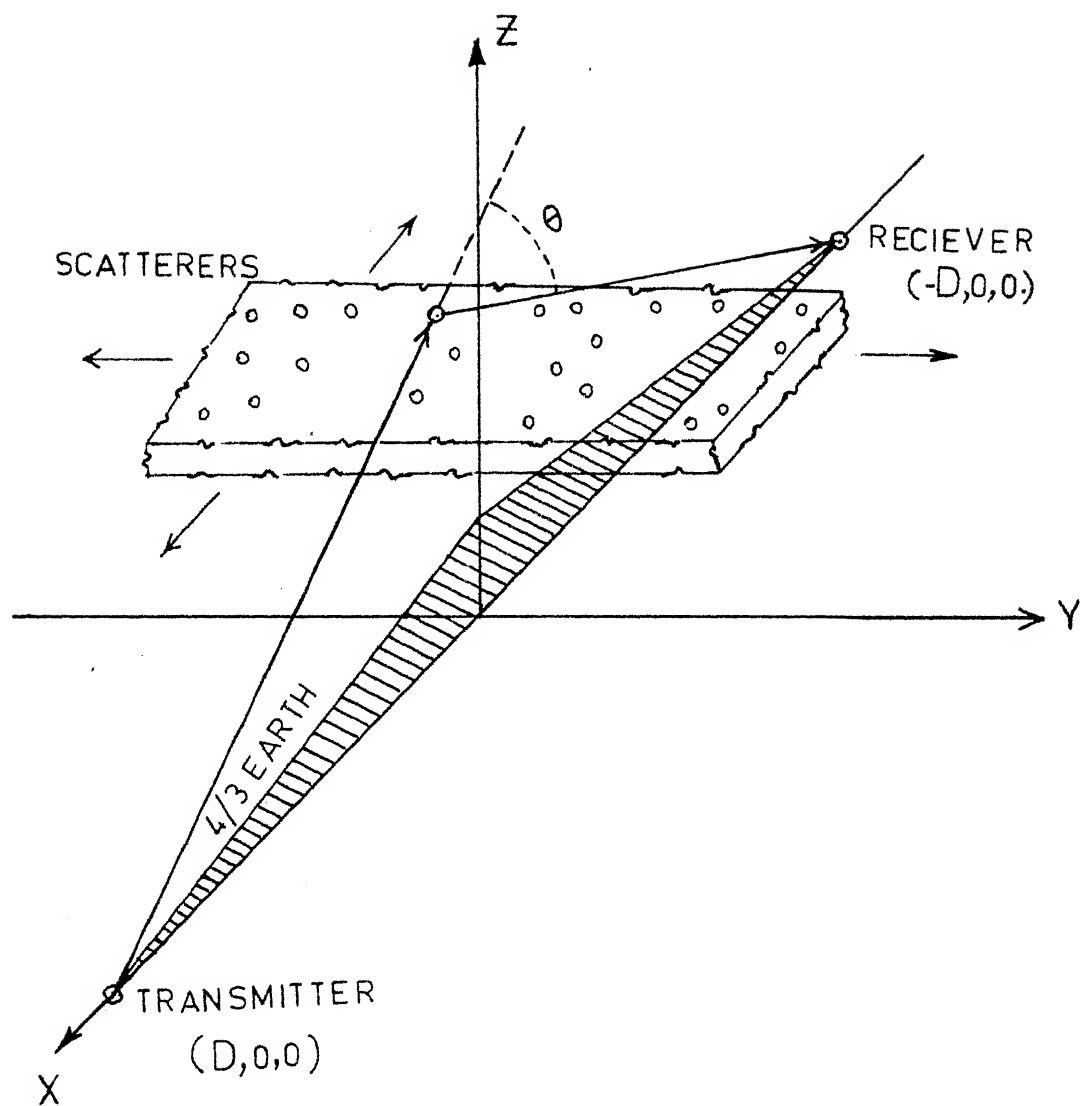


FIG. 4-1

If a  $\frac{4}{3}$  earth radius is employed to account for refraction effects, then surfaces of constant ray path length appear as ellipsoids of revolution about the chord line (X - axis) with the transmitter and receiver as focii. A transmitted signal received via any single moving scatterer is shifted in frequency by a small amount, proportional to the rate at which the scatterer crosses the constant ray path surfaces. The doppler shift  $f_D$  is given by

$$f_D = - \frac{1}{\lambda} \frac{dL}{dt} \quad (4.2)$$

Substituting (4.1) in (4.2)

$$f_D = - \frac{4 uX(1-4D^2/L^2) + VY + WZ}{(1-16 X^2 D^2/L^4) \lambda L} \quad (4.3)$$

where

$$u = \frac{dX}{dt}, \text{ along path wind speed}$$

$$V = \frac{dY}{dt}, \text{ cross path wind speed}$$

$$W = \frac{dZ}{dt}, \text{ vertical wind speed}$$

Since, the factor  $(1 - 4D^2/L^2)$  is small, the along path wind speed contributes very little to  $f_D$ . Therefore,

scatterers that move in a direction perpendicular to the midpath plane and parallel to the constant ray path length surfaces contribute very little to doppler shift of the received signal. The vertical winds are usually much smaller than the horizontal winds. Essentially all received signal variation is due to cross path horizontal scatterer movement. Therefore, the layered, drifting with wind, discrete scatterer model of tropospheric scatter can be simplified for purpose of simulation through the assumption that scatterers exist only in the midpath plane.

Assuming that the crosspath wind speed is much greater than the vertical speeds, then (4.3) becomes

$$\begin{aligned}
 f_D &= - \frac{2}{\lambda} V \left( \frac{2Y}{L} \right) \\
 &= - \frac{2}{\lambda} V \sin \alpha \\
 &= - \frac{2}{\lambda} V \alpha
 \end{aligned} \tag{4.4}$$

where  $\alpha$  is the azimuthal angle of the scattering point from the great circle plane.

The propagation time delay,  $\tau(X,Y,Z)$  associated with each scatterer, relative to the shortest, or earth grazing ray path is given by



$$\tau(X,Y,Z) = \frac{1}{C} [L(X,Y,Z) - L(0,0,Z_G)] \quad (4.5)$$

where  $(0,0,Z_G)$  is the point where the grazing ray intersects the Z axis as shown in Fig. 4.1 and C is the speed of light. The surfaces of constant path length can also be described as surfaces of constant time delay. Then, the doppler shift  $f_D$  can be written in terms of delay  $\tau$ , given by

$$f_D = -f_c \frac{d\tau}{dt} \quad (4.6)$$

where  $f_c$  = frequency of the transmitted signal.

The common volume can be divided into concentric shells of constant path delay increments as illustrated in Fig. 4.2. At midpath plane for  $X = 0$ , from (4.5)

$$\begin{aligned} \tau &= \frac{L(0,Y,Z) - L(0,0,Z_G)}{C} \\ &= \frac{2[(D^2+Y^2+Z^2)^{\frac{1}{2}} - (D^2+Z_G^2)^{\frac{1}{2}}]}{C} \end{aligned}$$

or,

$$\frac{C\tau}{2} = (D^2+Y^2+Z^2)^{\frac{1}{2}} - (D^2+Z_G^2)^{\frac{1}{2}}$$

or,

$$(D^2+Y^2+Z^2)^{\frac{1}{2}} = \frac{C\tau}{2} + (D^2+Z_G^2)^{\frac{1}{2}}$$

or,

$$Y^2+Z^2 = \left[ \frac{C\tau}{2} + (D^2+Z_G^2)^{\frac{1}{2}} \right]^2 - D^2 \quad (4.7)$$

The equation (4.7) is a circle on Y,Z plane ; on the right hand side of the equation the only variable is the delay  $\tau$ . So by changing the values of constant delay  $\tau$  the radius of the circle on Y,Z plane changes. For any constant delay  $\tau$  , if the radius of the circle is R then R is given by

$$R^2 = \left[ \frac{C\tau}{2} + (D^2 + Z_G^2)^{\frac{1}{2}} \right]^2 - D^2 \quad (4.8)$$

By simulating the link parameters and the common volume geometry of Kanpur - Nainital troposcatter link, the constant delay shells are illustrated in Fig. 4.2.

Delay increments of 0.025  $\mu$ secs is given in the simulation program.

#### 4.2 Antenna Gain Pattern and Off Set Effects

The signal voltage observed at a scatterer resulting from a signal transmitted from a narrow beam-width antenna is a function of the antenna radiation pattern through the angular relationship between the signal ray path to the scatterer and the bore-sight line of maximum gain of the transmitting antenna. A similar angular relationship holds between the signal ray path from the scatterer to the receiving antenna and the maximum gain boresight line for this antenna. Then the gain pattern

effect upon received signal voltage for a single scatterer is given by

$$A_N(\alpha_T, \alpha_R) = G_T(\alpha_T) G_R(\alpha_R) \quad (4.9)$$

where

$\alpha_T$  = angle between transmitted signal ray path to scatterer and bore-sight direction of the transmitting antenna

$\alpha_R$  = angle between received signal ray path from scatterer and the bore-sight direction of the receiving antenna.

For this simulation work, a Gaussian circular gain pattern for both transmitter and receiver antennas is assumed. Then antenna gain pattern and off set effects is given by a function (G) as under as explained at Section 2.3.

$$G = \text{Exp} [-(Y - Y_c)^2 / Y_m^2] \quad (4.10)$$

#### 4.3 Angular Dependence Function

For isotropic turbulence, if a single scattering layer exists in the common volume, its edge on view would be super imposed on the ellipsoidal cross section

as shown in Fig. 4.2. The scattering cross section  $\sigma(\theta)$  as a function of scattering angle  $\theta$  is of interest since it determines how the reflectivity of scattering structure varies with position.

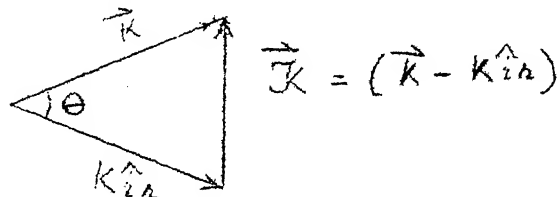
The scattering cross section per unit volume  $\sigma(\theta)$  is the power scattered towards the receiver per unit volume per unit solid angle per unit incident power density. This is given by (Tatarski [7])

$$\sigma(\theta) = 2\pi K^4 \sin^2 \chi \Phi(\vec{K} - K\hat{i}_n) \quad (4.11)$$

where  $\chi$  = angle between the electric field intensity of the incident plane wave and the direction of the receiver

$\Phi(\vec{K} - K\hat{i}_n)$  = spectrum of refractivity fluctuations

The vector  $(\vec{K} - K\hat{i}_n)$  is defined as shown in the Figure below.



And the vector  $K = \vec{K} - K\hat{i}_n$  has a magnitude given by

$$K = 2K \sin \frac{\theta}{2} \quad (4.12)$$

For isotropic turbulence model, based on Tatarski's theory (7), the spectrum of refractive index fluctuations due to turbulence is given by

$$\bar{\phi}(K) = 0.033 \text{ Cn}^2 (K)^{-p} \quad (4.13)$$

where  $\text{Cn}^2$  = refractive index structure function coefficient

$p = \frac{11}{3}$  for Tatarski's model which is now generally accepted

This leads to a scattering cross section.

$$\sigma(\Theta) = 2\pi K^4 \sin^2 \frac{\Theta}{2} \times 0.033 \text{ Cn}^2 (2K \sin \frac{\Theta}{2})^{-p} \quad (4.14)$$

For small scattering angles,  $\Theta$  can be written in terms of the paths' chord length  $2D$ , the height of the scattering point  $Z$  and the cross path displacement of the scattering point  $y$

$$\begin{aligned} \frac{\Theta}{2} &= \tan^{-1} \left[ \frac{(Y^2 + Z^2)^{\frac{1}{2}}}{(D-X)} \right] + \tan^{-1} \left[ \frac{(Y^2 + Z^2)^{\frac{1}{2}}}{(D+X)} \right] \\ &= \left[ \frac{Y^2 + Z^2}{D^2} \right]^{\frac{1}{2}} \quad \text{for } X \ll D \end{aligned}$$

$$\begin{aligned}
\sigma(\theta) &\propto \sin^{-p} \left[ \frac{Z^2 + Y^2}{D^2} \right]^{\frac{1}{2}} \\
&\propto \left[ \frac{Z^2 + Y^2}{D^2} \right]^{-p/2} \\
&\propto \left[ \frac{D^2}{Z^2 + Y^2} \right]^{p/2}
\end{aligned} \tag{4.15}$$

For Tatarski's model, the scattering cross  $\sigma(\theta)$  is given by

$$\sigma(\theta) \propto \left[ \frac{D^2}{Y^2 + Z^2} \right]^{11/6}$$

In this simulation work  $p = 2, 11/3, 5$  are considered in obtaining the delay, doppler power spectra. Birkemeier [3] has designated this scattering angle dependence as the angular dependence function. When a layer of some thickness is considered,  $Z$  in (4.15) is taken as the average height of the scatterers called  $Z_0$ , then  $\sigma(\theta)$  is given by

$$\sigma(\theta) \propto \left[ \frac{D^2}{Y^2 + Z_0^2} \right]^{\frac{p}{2}} \tag{4.16}$$

When the turbulence is anisotropic with the horizontal correlation distance greater than the vertical correlation distance, then the angular dependence is written as

$$\sigma(\theta) \propto \left[ \frac{D^2}{A^2 Y^2 + Z_o^2} \right]^{\frac{p}{2}}, \quad \Lambda > 1 \quad (4.17)$$

model

For Tatarski's (4.17) becomes

$$\sigma(\theta) \propto \left[ \frac{D^2}{A^2 Y^2 + Z_o^2} \right]^{\frac{11}{6}}$$

#### 4.4 Ambiguity Function

Measurement of the scattering function of a time and frequency - spread tropo-channel requires an input signal having an ambiguity function that is very narrow in both time and frequency co-ordinates. Otherwise the measured impulse response of the tropo-channel will be smeared due to the ambiguity function of the input signal. The signal used in the Rake System, a carrier that is phase shift modulated by a long PN sequence, is an ideal probe signal. By choosing, very small length of a single modulating pulse ( $\tau_o$ ) and very large repetition period  $(T_o)$  of the PN sequence, we can have the ambiguity function reasonably close to an impulse. Therefore, the measured scattering function which is the convolution of the true scattering function and ambiguity function can be taken as the true scattering function. In other words, smearing of the ambiguity function is ignored.

In this work, the parameters  $\tau_0$  and  $T_0$  are taken as 0.1 microsecs and 3.2767 millisecs respectively, thus making the ambiguity function reasonably close to an impulse. In this simulation work, the ambiguity function (Af) is considered unity by choosing the above values of the parameters  $\tau_0$  and  $T_0$ .

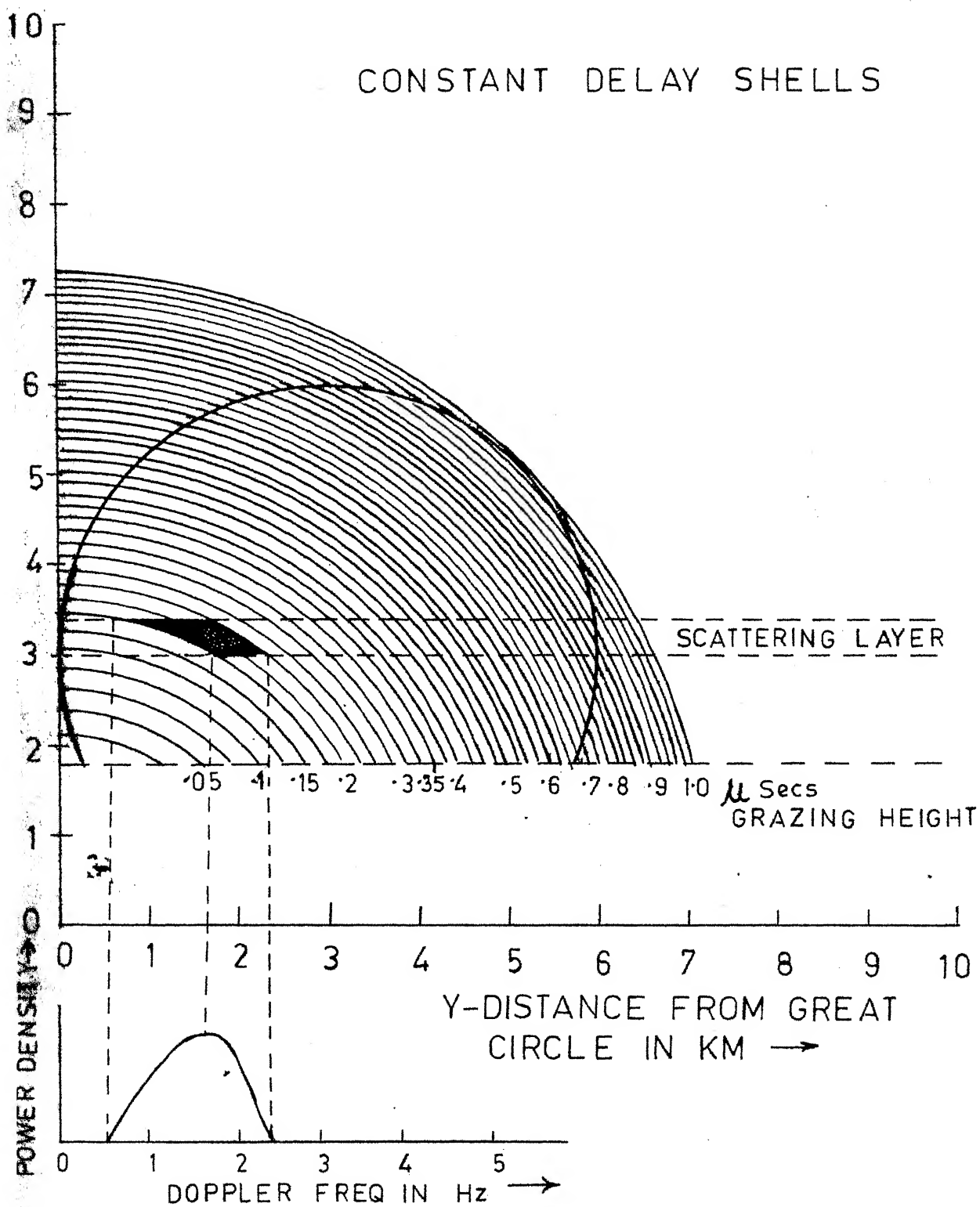
#### 4.5 Magnitude Weighting Function $M(\ell)$

In order to account for the possibility of layers at different heights having different scattering strengths a magnitude weighting function  $M(\ell)$ , whose value is different but constant for each layer is used. However,  $M(\ell)$  is considered unity when single scattering layer is simulated in this work. For multiple scattering layers only, we have considered different weightings for different layers.

#### 4.6 Delay Shell - Scattering Volume

We have seen that the doppler frequency is proportional to the off - great circle displacement ( $y$  - displacement). A first order estimate of the shape of the delay, doppler spectra can therefore be made from the relative portion of scattering volume available as a function of doppler frequency (or  $y$ ). In Fig. 4.2 by introducing an hypothetical scattering layer at a height of 3 KMS and of thickness 400 Mtrs, we can visualize the scattering area subtended by the





scattering layer for any delay shell. For example let us consider the scattered power density at Rake tap No.4 for relative multipath delay of 0.2 microsec. The scattering power seen by the Rake tap No.4 is due to scattering from the shaded area i.e. the area subtended by the scattering layer and constant delay shells of 0.175 microsecs and 0.225 microsecs as shown in Fig. 4.2. The resultant scattered power density as function of doppler shift is shown in Fig. 4.2 based on the area within a certain doppler frequency range.

The area subtended by the scattering layer and the constant delay shells is computed as under :

- (a) For the region ABC in Fig. 4.3, the area is proportional to Z axis length subtended by the delay shell having radii  $R_1$  and  $R_2$ .

For radius  $R_1$ ,  $Z_1$  is given by

$$Z_1 = \sqrt{(R_1^2 - Y^2)}$$

$$\begin{aligned} \therefore \text{Area} &= SH_2 - Z_1 \\ &= SH_2 - \sqrt{(R_1^2 - Y^2)} \end{aligned} \quad (4.20)$$

- (b) For the region BCDE, area is given by

$$\text{Area} = SH_2 - SH_1 \quad (4.21)$$

(c) In the region DEF, area is again proportional to the Z axis length subtended by the delay shell

For radius  $R_2$ ,  $Z_2$  is given by

$$Z_2 = \sqrt{(R_2^2 - Y_2^2)}$$

$$\therefore \text{Area} = \sqrt{(R_2^2 - Y^2)} - SH_1 \quad (4.22)$$

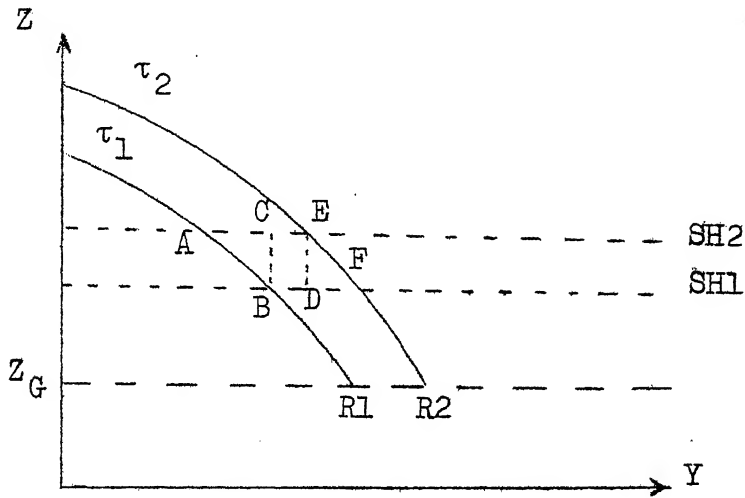


Figure 4.3

#### 4.7 Discussion

The delay doppler power spectral density simulated in this work is a function of the following factors discussed in brief in the foregoing sections : -

- (a) Scattering cross section or angular dependence function  $\sigma(\theta)$ , given by

$$\sigma(\theta) = \left[ \frac{D^2}{A^2 Y^2 + Z_0^2} \right]^{\frac{P}{2}}$$

(b) Antenna gain pattern  $G$ , given by

$$G = \text{Exp} - [(Y - Y_c)^2 / Y_m^2]$$

(c) Area subtended by the scattering layer and the particular Rake tap delay shell

(d) Ambiguity function  $A_f$ , which is considered unity.

(e) Magnitude weighting function  $M(\ell)$ , which is considered unity for a single scattering layer simulations. For multiple scattering layers simulation, different integer values are considered for each layer as weighting function.

For a single scattering layer, the amplitude of the delay doppler power spectral density is given by

$$\text{Amplitude} = \sigma(\theta) \times G \times \text{Area} \quad (4.23)$$

For a multiple scattering layers, the amplitude of the delay doppler power spectral density as given by

$$\text{Amplitude} = \sigma(\theta) \times G \times \text{Area} \times M(\ell) \quad (4.24)$$

is used for simulation work.

## CHAPTER 5

## SCATTERING FUNCTIONS - DELAY, DOPPLER POWER SPECTRA

5.1 Delay, Doppler Locus for a Single Layer

The delay doppler power spectral density for relative multipath delays of 0.05 microsecs to 0.95 microsecs are illustrated in Figs. 5.2 through 5.25. In these figures we notice the parabolic trace that a layer produces in a scattering function. The parabola results from the fact that the multipath delay in the signal received from a point scatterer varies as the square of the cross path position, while the doppler frequency varies linearly with cross path position. This is shown as follows :

For a layer at height  $Z$ , we wish to find the delay  $\tau$  as we move along the layer in the cross path direction  $Y$ . Since the constant delay surfaces are circles,  $\tau$  will not vary along the surface defined by the radius  $\sqrt{Z^2 + Y^2}$

From equation (4.7)

$$\tau(0,Y,Z) = \frac{2}{C} [(D^2+Y^2+Z^2)^{\frac{1}{2}} - (D^2+Z^2)^{\frac{1}{2}}] \quad (5.1)$$

$$\begin{aligned}
\tau(O, Y, Z) &= \frac{2}{C} \left[ D \left( 1 + \frac{Y^2 + Z^2}{D^2} \right)^{\frac{1}{2}} - D \left( 1 + \frac{Z_G^2}{D^2} \right)^{\frac{1}{2}} \right] \\
&= \frac{2}{C} \left[ D \left\{ 1 + \frac{1}{2} \left( \frac{Y^2 + Z^2}{D^2} \right) \right\} - D \left( 1 + \frac{1}{2} \frac{Z_G^2}{D^2} \right) \right] \\
&= \frac{2}{C} \left[ \frac{Y^2}{2D} + \frac{Z^2}{2D} - \frac{Z_G^2}{2D} \right] \quad (5.2)
\end{aligned}$$

Substituting the doppler shift relation (4.4)  $f_D = \frac{4 VY}{\lambda L_0}$ , where  $L_0$  is the grazing ray path length which is approximately equal to  $2D$

$$f_D = \frac{2 VY}{\lambda D}$$

or

$$Y = \frac{f_D \lambda D}{2 V} \quad (5.3)$$

Substituting equation (5.3) in equation (5.2), we have

$$\tau(O, Y, Z) = \frac{f_D^2 \cdot \lambda^2 \cdot D}{4 V^2 \cdot C} + \frac{Z^2}{C \cdot D} - \frac{Z_G^2}{C \cdot D}$$

By substituting the Kanpur - Nainital troposcatter link parameters and the geometry, we have

$$\tau(O, Y, Z) = 2.8 \frac{f_D^2}{V^2} + \frac{Z^2}{49.5} - .0655 \quad (5.4)$$

where  $\tau$  is in microsecs

$V$  is in metrs/sec

$Z$  is in kms ;  $f_D$  is in Hz

A cross path wind velocity ( $V$ ) of 11.8 metres/sec is assumed for the simulation work.

Equation (5.4) gives the delay - doppler locus for a single layer.

## 5.2 Simulation of Scattering Functions

The scattering function is a plot of the power spectral density as a function of doppler frequency shift for each value of propagation delay  $\tau$ . Scattering functions are simulated based on the simulation model developed in Chapter 4 to illustrate the effects of antenna azimuth off set, antenna elevation off set, types of layers and power index  $p$  of the power law spectra.

Digital computer simulation programs are written in Fortran IV source language which are processed by IBM-1800 digital computer and the scattering functions are plotted by IBM-1627 plotter. The listings of these programs are given at Appendix A. A series of simulation results in the form of scattering functions are obtained in Figures 5.2 through 5.25.

To facilitate the discussion of scattering functions results, the figures are divided into seven sets based on antenna off set angles, number of layers and thickness of scattering layer.

NOTE : - The scale factor of relative power density has been changed for each figure in each set to display the lower spectral levels more clearly.

#### 5.2.1 Scattering functions : Set - 1

The scattering function results of this set correspond to the simulation set up shown in Fig. 5.1 . The simulation program listings for Fig. 5.1 and for Figs. 5.2 through 5.4 are given at appendix A-1 and A-2 respectively. The salient simulation parameters are given as under :

- a) Antenna off set ( $Y_c$ ) = 0
- b) Single scattering layer at a height ( $SH_1$ ) = 3 KMS
- c) Scattering layer thickness ( $SH_2 - SH_1$ ) = 400 Mtrs
- d)  $p = 2, \frac{11}{3}, 5$
- e) Isotropic layer ( $\Lambda = 1$ )
- f) Gaussian circular antenna pattern of 3 KMS radius at the midpath plane

The resulting scattering functions are illustrated in Figs. 5.2 through 5.4. The following observation are made :

- a) The more apparent effect of increasing the value of  $p$  is the increase in power received. This is because as  $p$  increases the scattering cross section increases governed by equation (4.16).



## CONSTANT DELAY SHELLS

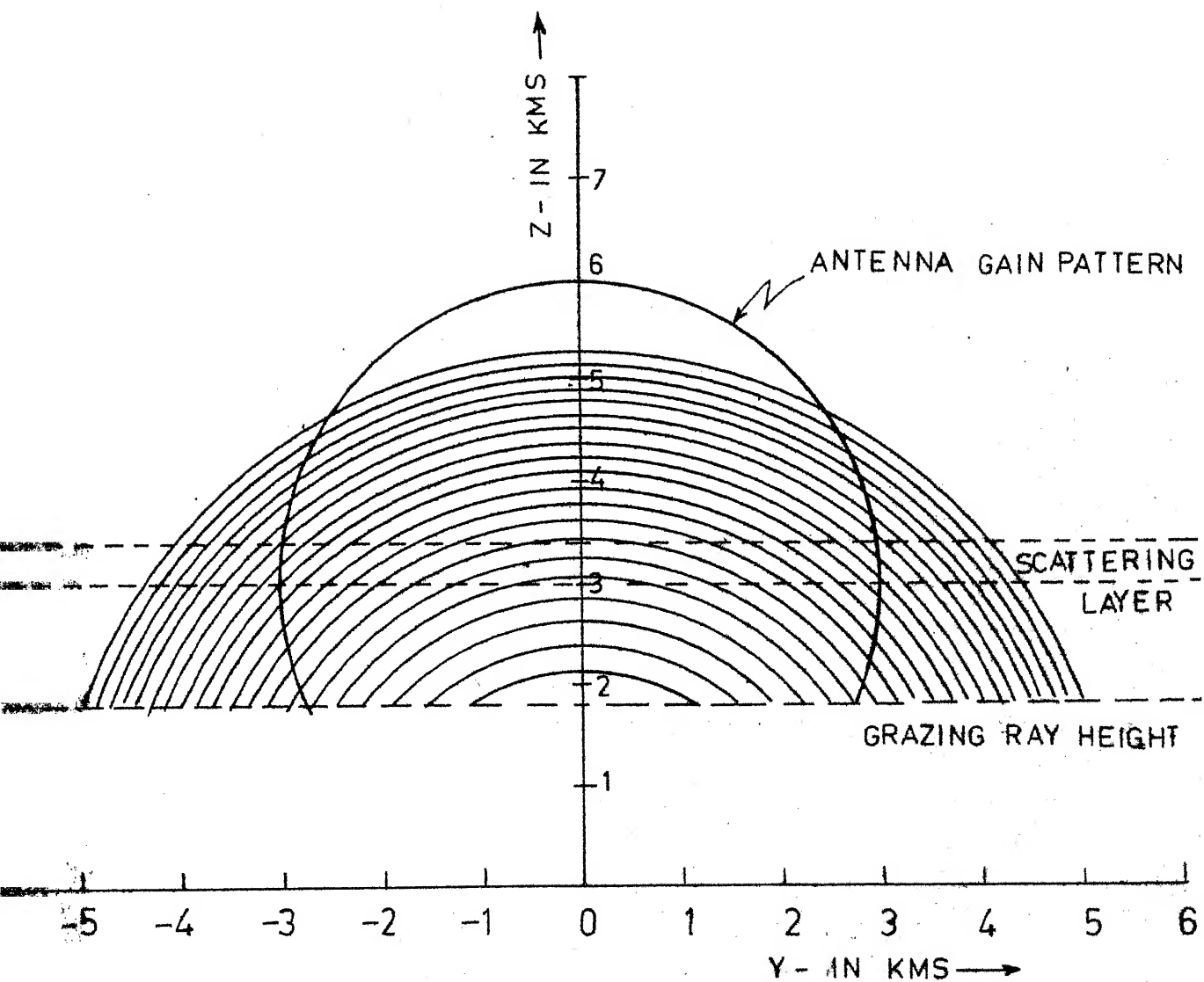


FIG. 5-1

DELAY-DOPPLER POWER SPECTRA: FOR  
NO ANTENNA OFFSET  $Y_c = 0$  Kms

$SH_1 = 3.0$  Kms

$SH_2 = 3.4$  Kms

$P = 11/3$

Scale:  $AMT = 10^{-5} \times AMT$

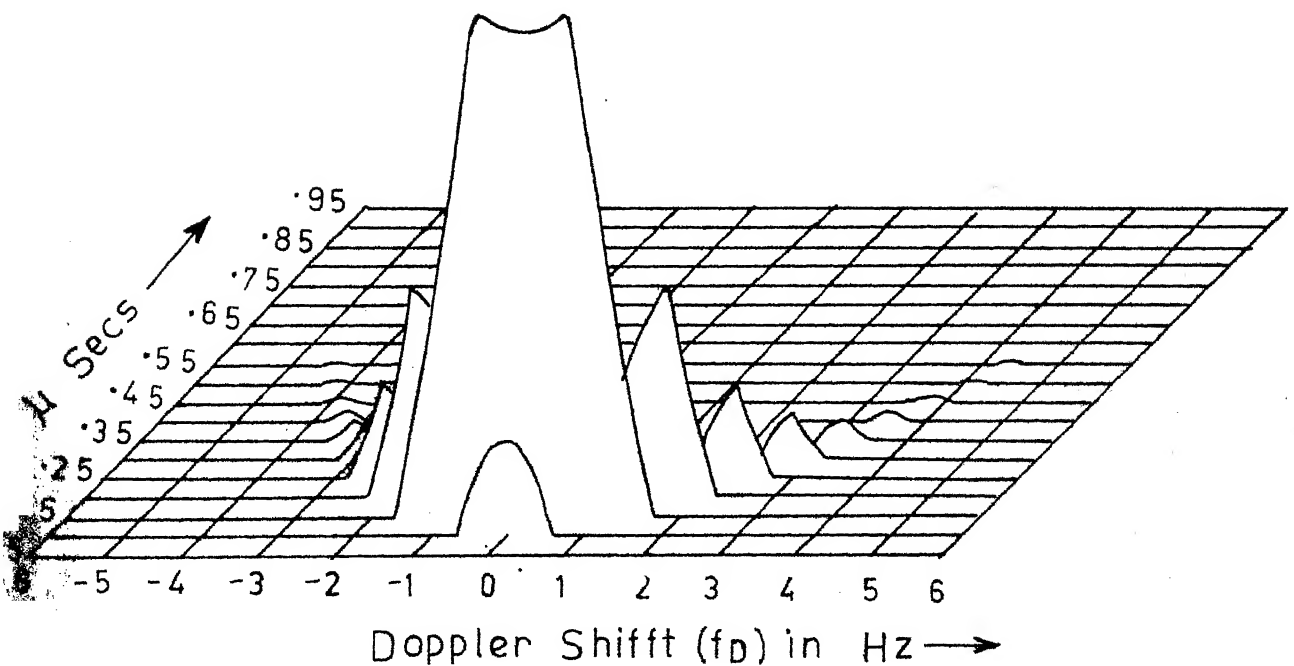


FIG.5-2

# DELAY-DOPPLER POWER SPECTRA: FOR NO ANTENNA OFFSET

$$Y_c = 0$$

$$P = 2$$

$$SH_1 = 3 \text{ KMS}$$

$$SH_2 = 34 \text{ KMS}$$

$$\text{Scale: } AMT = 10^{-2} \times AMT$$

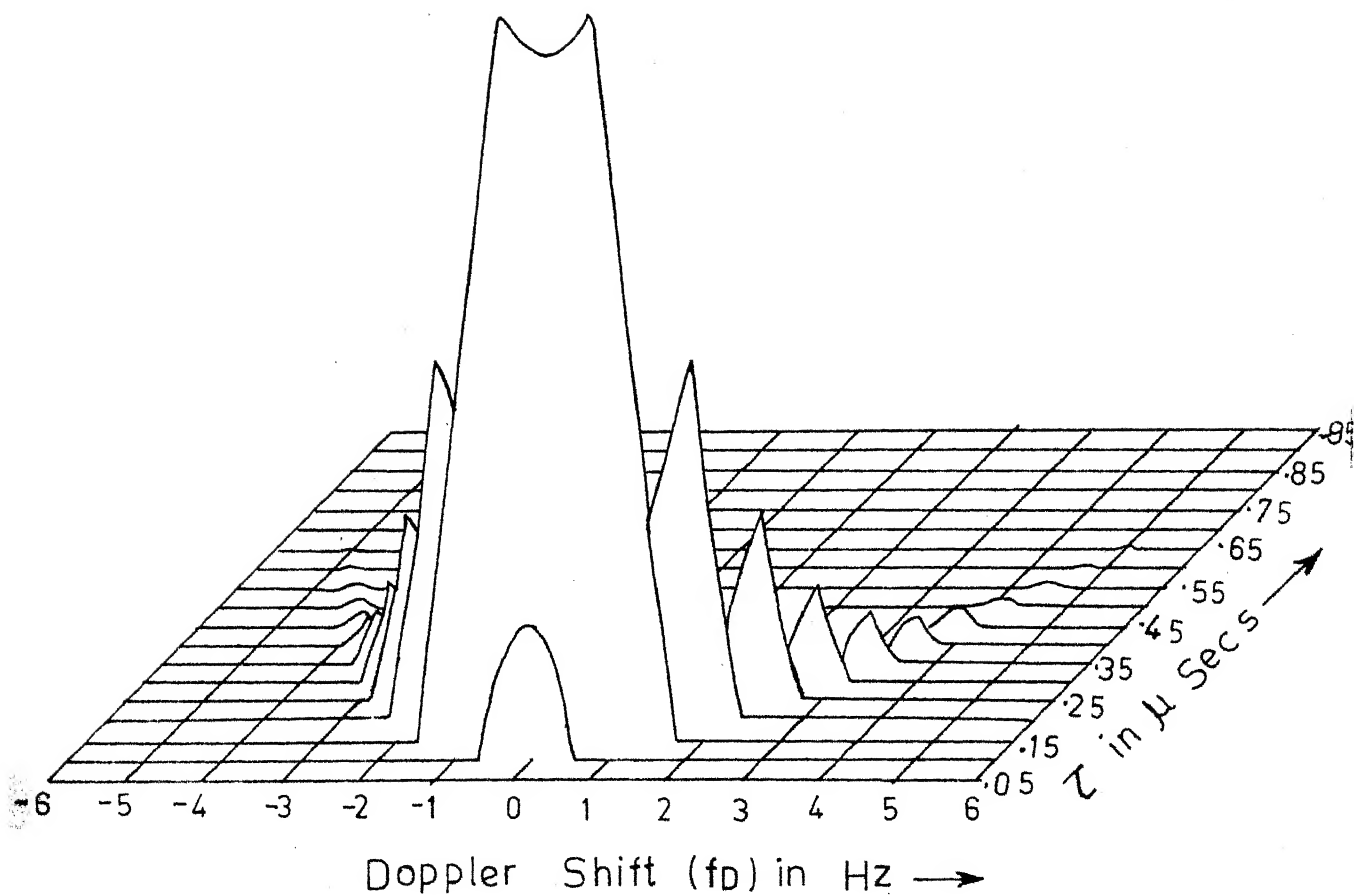
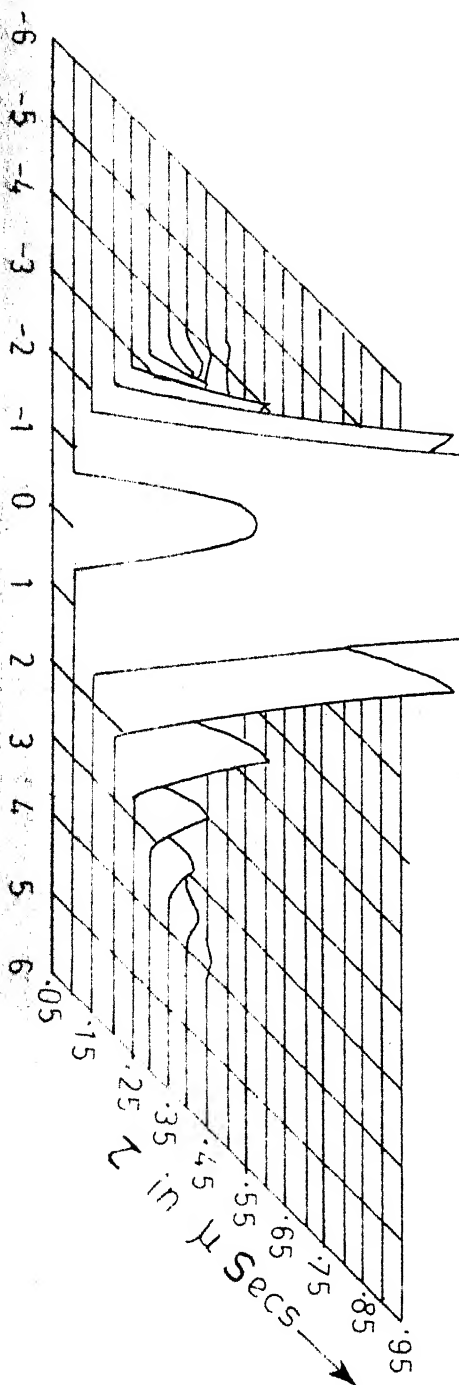


FIG. 5-3

# DELAY-DOPPLER POWER SPECTRUM: FOR NO ANTENNA OFFSET

$Y_C = 0$   
 $P = 5$   
 $SH_1 = 3 \text{ kms}$   
 $SH_2 = 3.4 \text{ kms}$   
 $\text{Scale: } \Delta MT = 10 \times \Delta MT^{-7}$



- b) Even though there are scatterers present in the assumed scattering layer in regions illuminated by antennas, where the relative delay is greater than 0.4 microsecs, the level of signals received at these greater delays is reduced considerably by the angular dependence function (4.16).
- c) Each of the figures of this set tends to illustrate the parabolic relationship of doppler frequency and multipath delay described by equation (5.4).

#### 5.2.2 Scattering functions - Set - 2

This set corresponds to the simulation set up shown in Fig. 4.2. The simulation program listings for Figs. 5.5 through 5.7 are given at Appendix (A-2). The important simulation parameters are given as under :

- a) Antenna azimuth off set ( $Y_0$ ) = 3 KMS
- b) Single scattering layer at a height ( $SH_1$ ) = 3 KMS
- c) Scattering layer thickness ( $SH_2 - SH_1$ ) = 400 Mtrs
- d)  $p = 2, \frac{11}{3}, 5$
- e) Isotropic layer ( $A = 1$ )
- f) Gaussian circular antenna gain pattern of 3 KMS radius at the midpath plane.

The resulting scattering functions are illustrated in Figs. 5.5 through 5.7. And the following observations are made : -

# DELAY-DOPPLER POWER SPECTRUM: ANTENNA AZIMUTH OFFSET BY 3 KMS

ANTENNA

$Y_c = 3 \text{ KMS}$   
 $P = 2$   
 $SH_1 = 3 \text{ KMS}$   
 $SH_2 = 3.4 \text{ KMS}$   
 Scale:  $AMT = 10^{-2} \times AM$

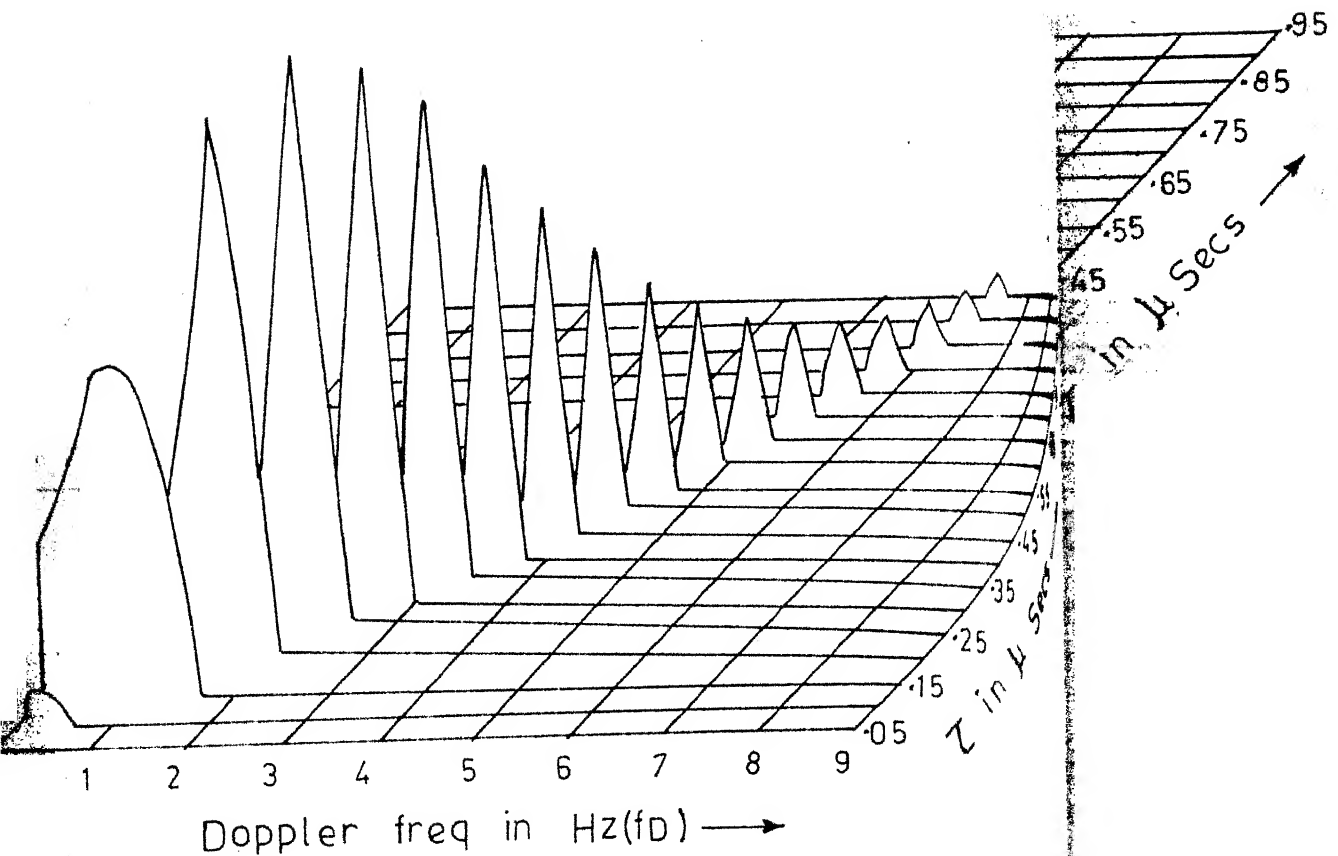


FIG. 5-5

~~DELAY~~-DOPPLER POWER SPECTRUM: ANTENNA  
AZIMUTH OFFSET BY 3 KMS

$Y_c = 3 \text{ KMS}$   
 $SH_1 = 3 \text{ KMS}$   
 $SH_2 = 3.4 \text{ KMS}$   
 $P = 11/3$   
 $A = 1^{-5}$   
 Scale:  $AMT = 10 \times AMT$

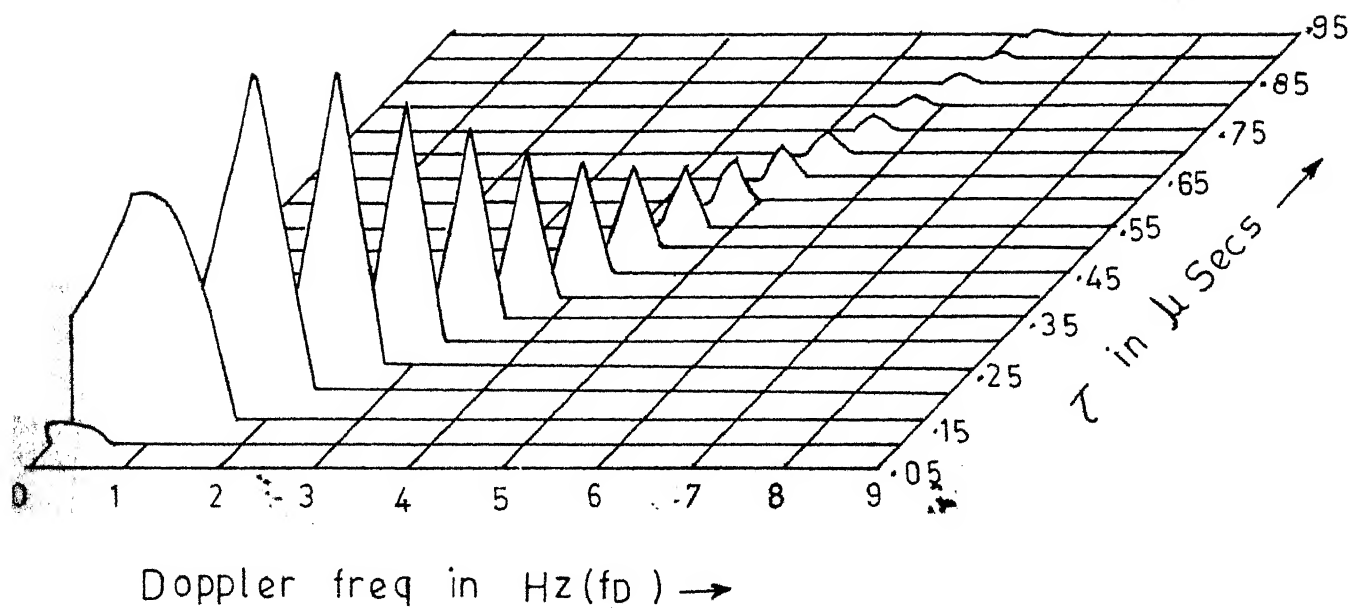


FIG. 5-6

# DELAY-DOPPLER POWER SPECTRUM: ANTENNA AZIMUTH OFFSET BY 3 KMS

$Y_c = 3 \text{ KMS}$   
 $P = 5$   
 $SH_1 = 3 \text{ KMS}$   
 $SH_2 = 3.4 \text{ KMS}$   
 Scale:  $AMT = 10^7 \times AMT$

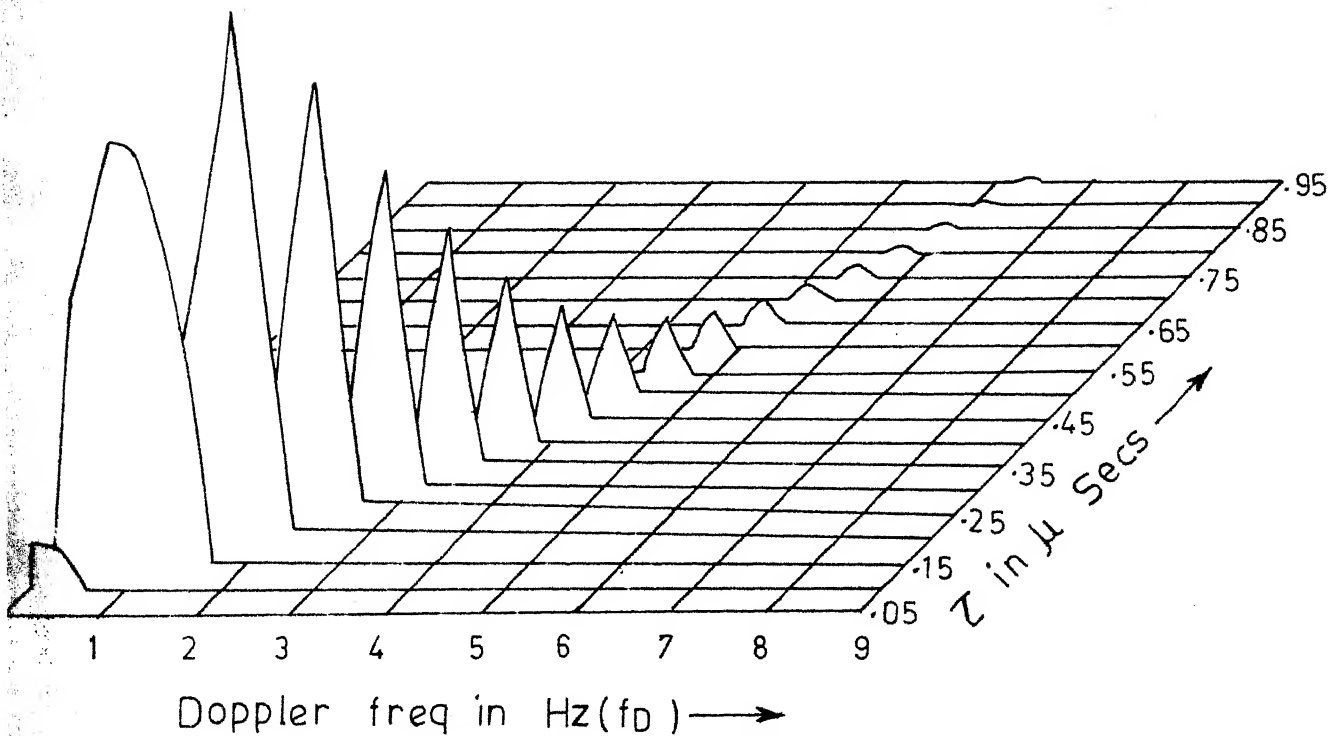


FIG. 5-7



- a) The scattered power density changes by antenna azimuth off set to a considerable extent.
- b) As the antenna off set is increased, signals received from the higher delay regions associated with the layer becomes more significant and signals from the lower delay regions are suppressed.
- c) Parabolic relationship between doppler frequency and multipath delay is justified
- d) The power density increases as the value of  $p$  increases
- e) The level of signals received for relative delays greater than 0.6 microsec is reduced due to the angular dependance function

### 5.2.3 Scattering functions : Set - 3

This set corresponds to the simulation set up. shown in Fig. 5.8. The important simulation parameters are as under :

- a)
  - a) Antenna azimuth off set ( $Y_0$ ) = 3 KMS
  - b) Antenna elevation off set = 1.8 KMS
  - c) Single scattering layer at a height ( $SH_1$ ) = 4.6 KMS
  - d) Scattering layer thickness ( $SH_2 - SH_1$ ) = 400 Mtrs
  - e)  $p = 2, \frac{11}{3}, 5$
  - f) Isotropic layer ( $A = 1$ )
  - g) Gaussian circular antenna gain pattern of 3 KMS radius at the midpath plane

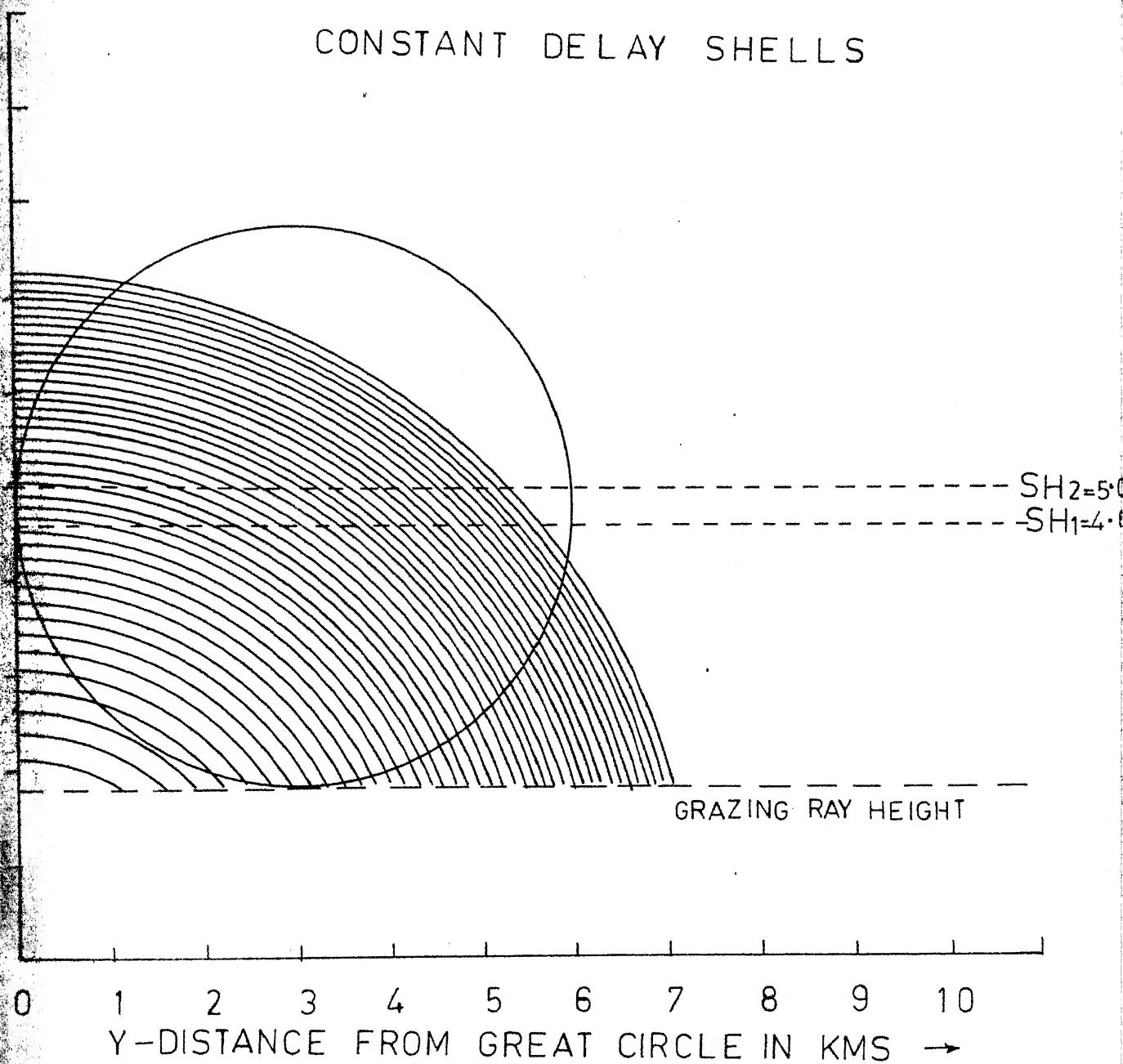


FIG.5-8

DELAY-DOPPLER POWER SPECTRUM: ANTENNA  
AZIMUTH OFFSET BY 3 KMS  
AND ELEVATION OFFSET BY 1.8 KMS

$$Y_c = 3 \text{ KMS}$$

$$P = 2$$

$$SH_1 = 4.6 \text{ KMS}$$

$$SH_2 = 5.0 \text{ KMS}$$

$$\text{Scale: } \text{AMT} = 10^{-2} \times \text{AMT}$$

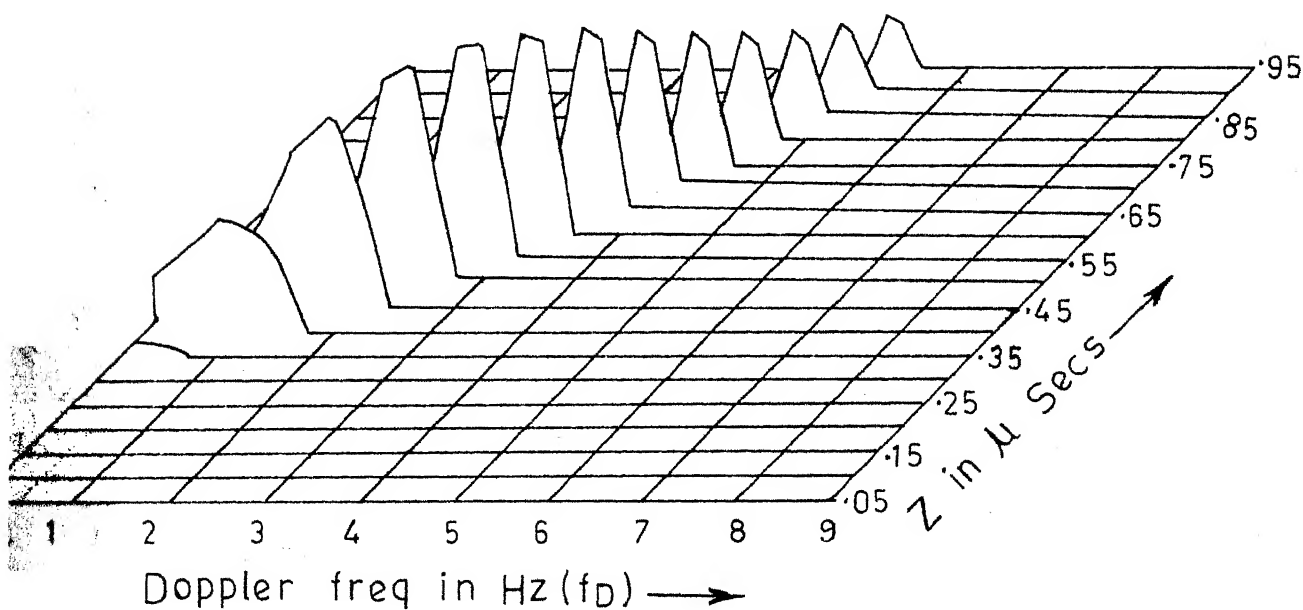


FIG. 5-9

DELAY DOPPLER SPECTRUM: ANTENNA  
AZIMUTH OFFSET BY 3 KMS AND  
ELEVATION OFFSET BY 1.8 KMS

$$Y_c = 3.0 \text{ KMS}$$

$$P = 11/3$$

$$SH_1 = 4.6 \text{ KMS}$$

$$SH_2 = 5.0 \text{ KMS}$$

$$\text{Scale: } \text{AMT} = 10^{-5} \times \text{AMT}$$

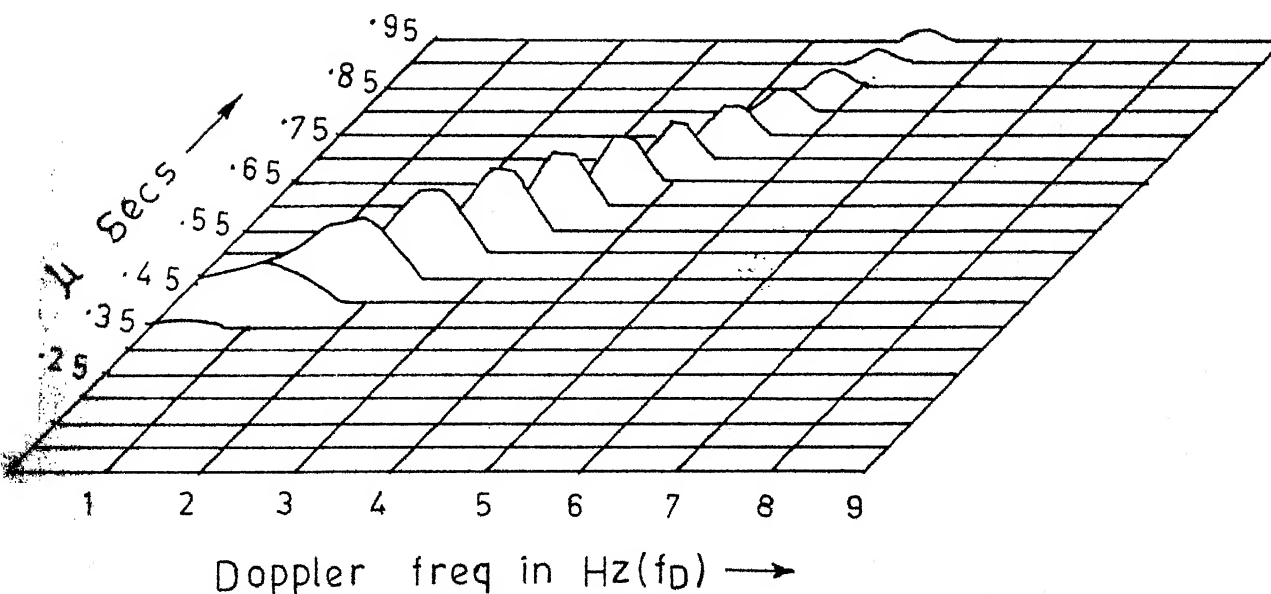


FIG. 5-10

DELAY-DOPPLER POWER SPECTRUM: ANTENNA  
AZIMUT OFFSET BY 3 KMS AND ELEVATION  
OFFSET BY 1.8 KMS

$Y_c = 3.0 \text{ KMS}$

$P = 5$

$SH_1 = 4.6 \text{ KMS}$

$SH_2 = 5.0 \text{ KMS}$

Scale:  $AMT = 10^{-7} \times AMT$

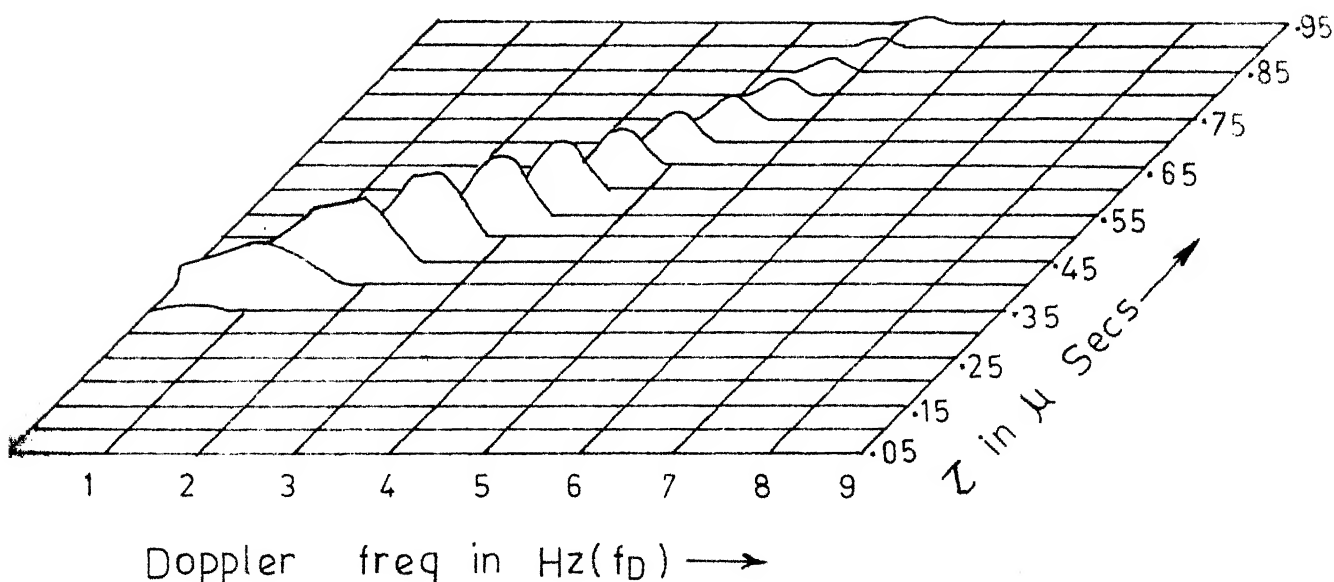


FIG. 5-11

The resulting scattering functions are illustrated in Figs. 5.9 through 5.11. The observations given in section 5.2.2 are valid. In addition the following are observed :

- a) For the same scale of Figs. 5.5 - 5.7 and 5.9 - 5.11 we notice a considerable reduction in the amplitudes of power spectrum for figs. at 5.9 - 5.11. This is because of elevation off set of the antennas.
- b) power received in the Rake taps from 1 to 6 is zero (for relative delay from .05 microsec to 0.3 microsec) due to the increase in layer height from where the scattering is assumed.
- c) The power spectral peaks are flat due to the constant area subtended by the scattering layer and the delay shells.

#### 5.2.4 Scattering functions : Set - 4

The simulation parameters are given as under :

- a) Antenna azimuth off set ( $Y_c$ ) = -3 KMS
- b) Single scattering layer at a height ( $SH_1$ ) = 3 KMS
- c) Scattering layer thickness = 400 Meters
- d)  $p = 2, \frac{11}{3}, 5$
- e) Isotropic layer ( $A = 1$ )
- f) Gaussian circular antenna gain pattern of radius 3 KMS at the mid path plane.

# DELAY-DOPPLER POWER SPECTRUM: ANTENNA AZIMUTH OFFSET BY -3 KMS

$Y_c = -3 \text{ KMS}$   
 $SH_1 = 3.0 \text{ KMS}$   
 $SH_2 = 3.4 \text{ KMS}$   
 $P = 2$   
 Scale:  $AMT = 10^{-2} \times AMT$

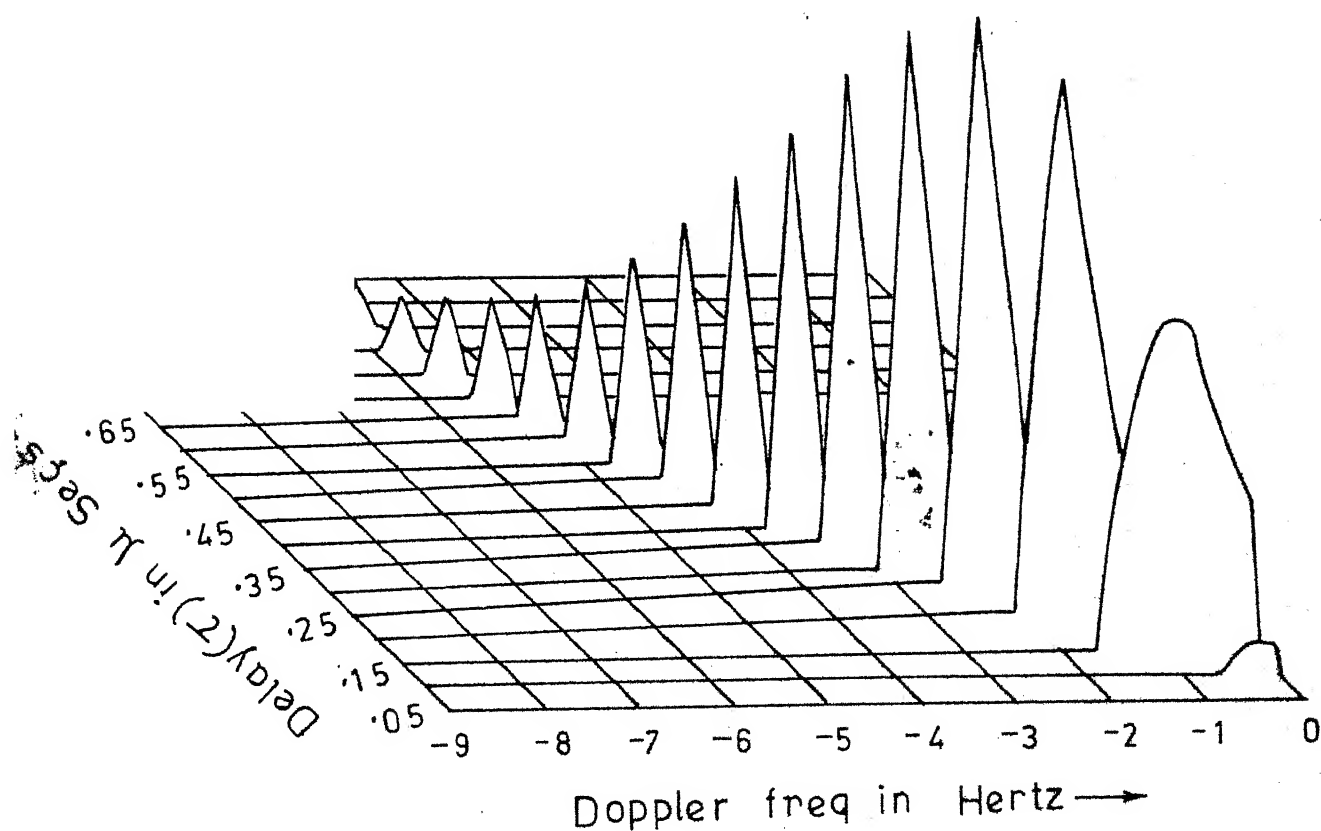


FIG. 5-12

DELAY-DOPPLER POWER SPECTRUM: ANTENNA  
AZIMUTH OFFSET BY -3 KMS

$Y_c = -3 \text{ KMS}$   
 $SH_1 = 3.0 \text{ KMS}$   
 $SH_2 = 3.4 \text{ KMS}$   
 $P = 11/3$   
 Scale:  $AMT = 10^{-5} \times AMT$

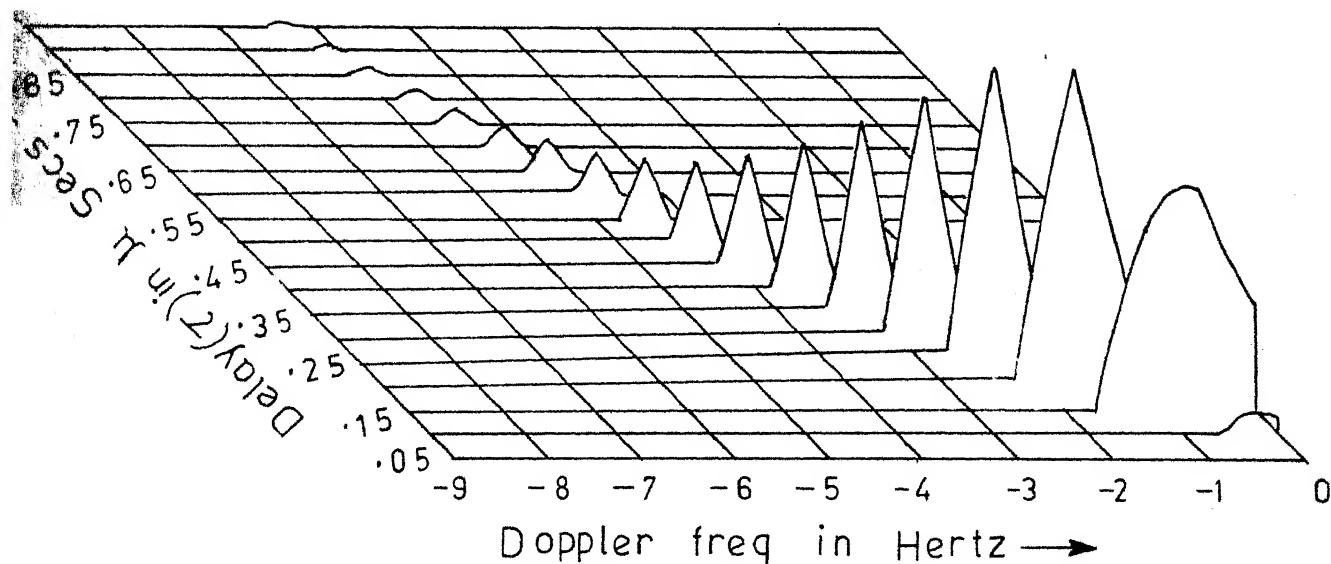


FIG. 5-13



DELAY-DOPPLER POWER SPECTRUM: ANTENNA  
AZIMUTH OFFSET BY -3 KMS

$Y_c = -3 \text{ KMS}$   
 $SH_1 = 30 \text{ KMS}$   
 $SH_2 = 3.4 \text{ KMS}$   
 $P = 5$   
 Scale:  $AMT = 10^{-7} X AMT$

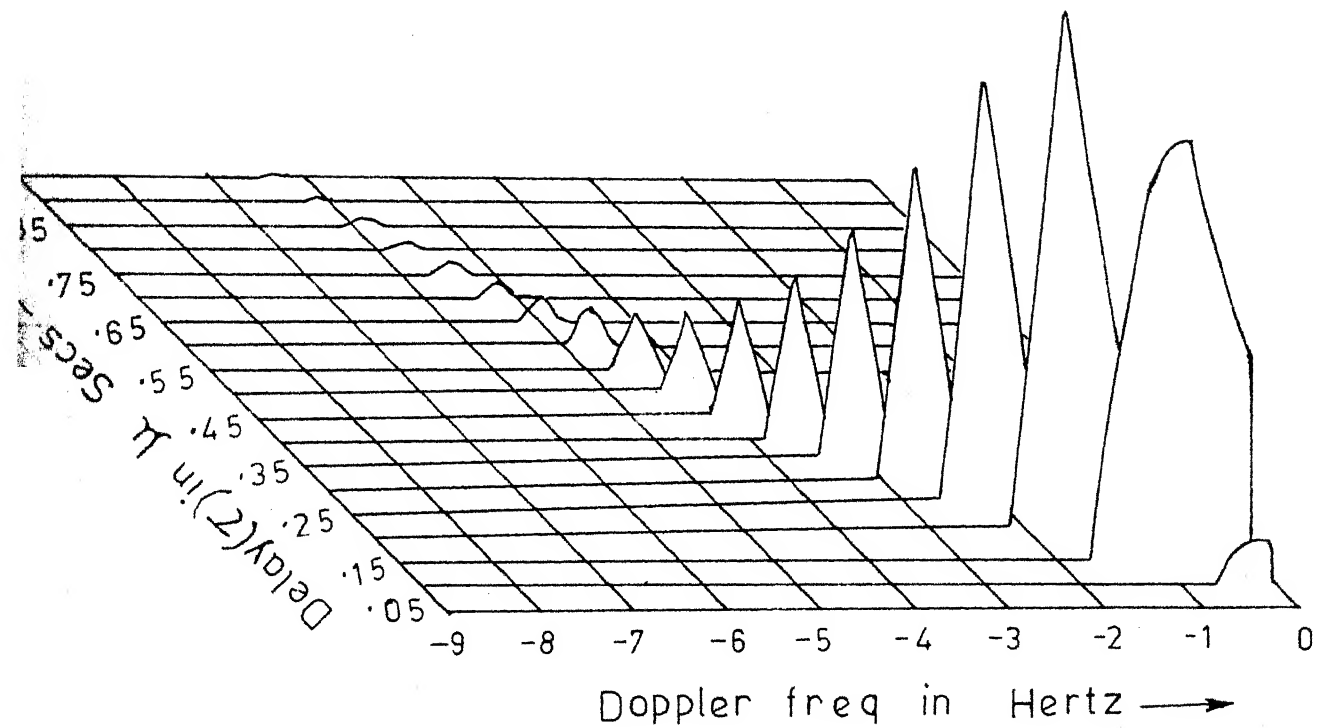


FIG. 5-14

DELAY DOPPLER POWER SPECTRUM ANTENNA  
AZIMUTH OFFSET BY -3KMS AND ELEVATION  
OFFSET BY 1.8 KMS

$$Y_c = -3 \text{ KMS}$$

$$P = 5$$

$$SH_1 = 4.6 \text{ KMS}$$

$$SH_2 = 5.0 \text{ KMS}$$

$$\text{Scale: } \text{AMT} = 10^{-7} \times \text{AMT}$$

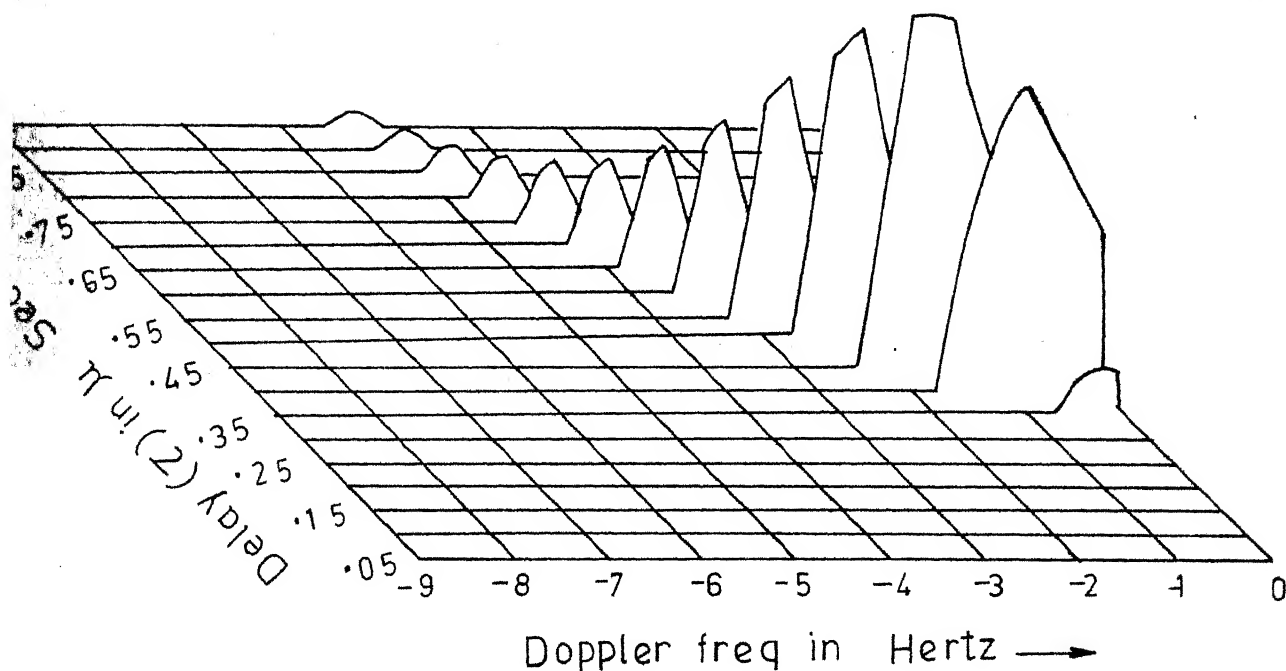


FIG. 5-17

DELAY DOPPLER POWER SPECTRUM ANTENNA  
AZIMUTH OFFSET BY -3 KMS AND ELEVATION  
OFFSET BY 1.8 KMS

$$Y_c = -3 \text{ KMS}$$

$$SH_1 = 4.6 \text{ KMS}$$

$$SH_2 = 5.0 \text{ KMS}$$

$$P = 2$$

$$\text{Scale: } \text{AMT} = 10^{-2} \times \text{AMT}$$

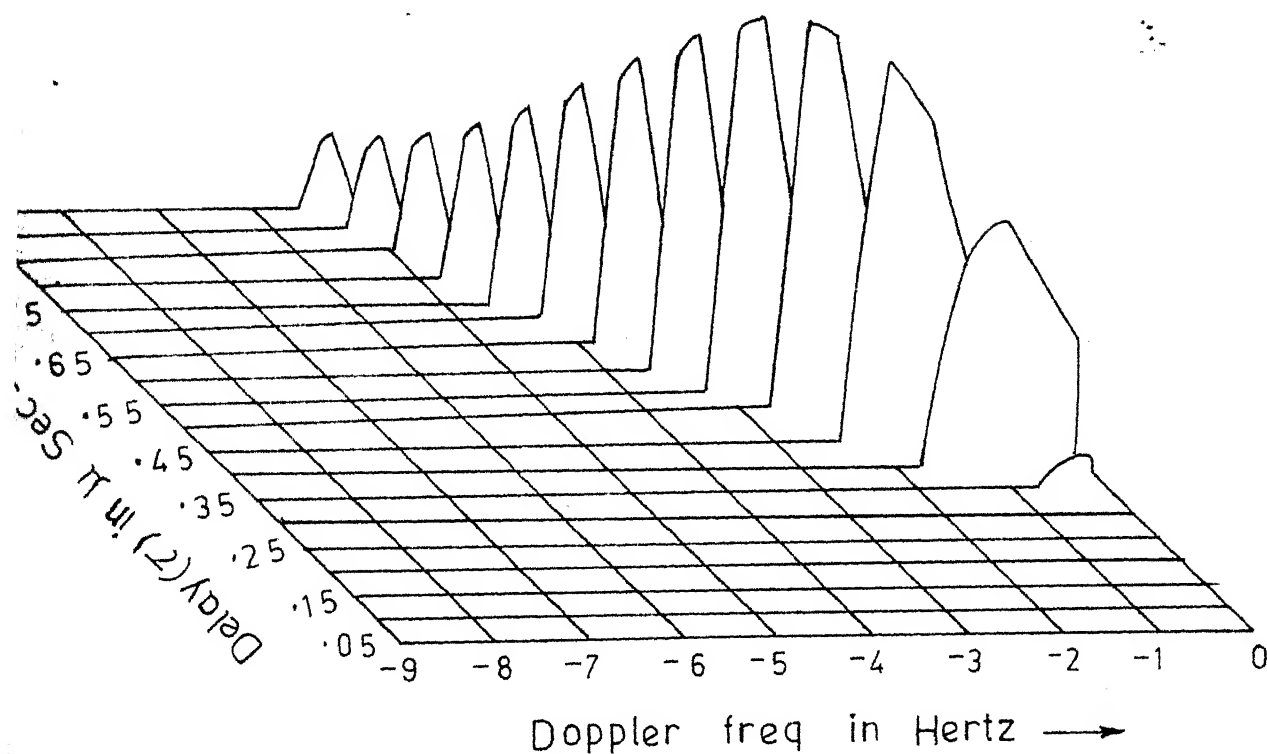


FIG. 5-15

DELAY-DOPPLER POWER SPECTRUM: ANTENNA  
AZIMUTH OFFSET BY -3 KMS AND ELEVATION  
OFFSET BY 1.8 KMS

$$Y_c = -3 \text{ KMS}$$

$$SH_1 = 4.6 \text{ KMS}$$

$$SH_2 = 5.0 \text{ KMS}$$

$$P = 11/3$$

$$\text{Scale: } \text{AMT} = 10^{-5} \times \text{AMT}$$

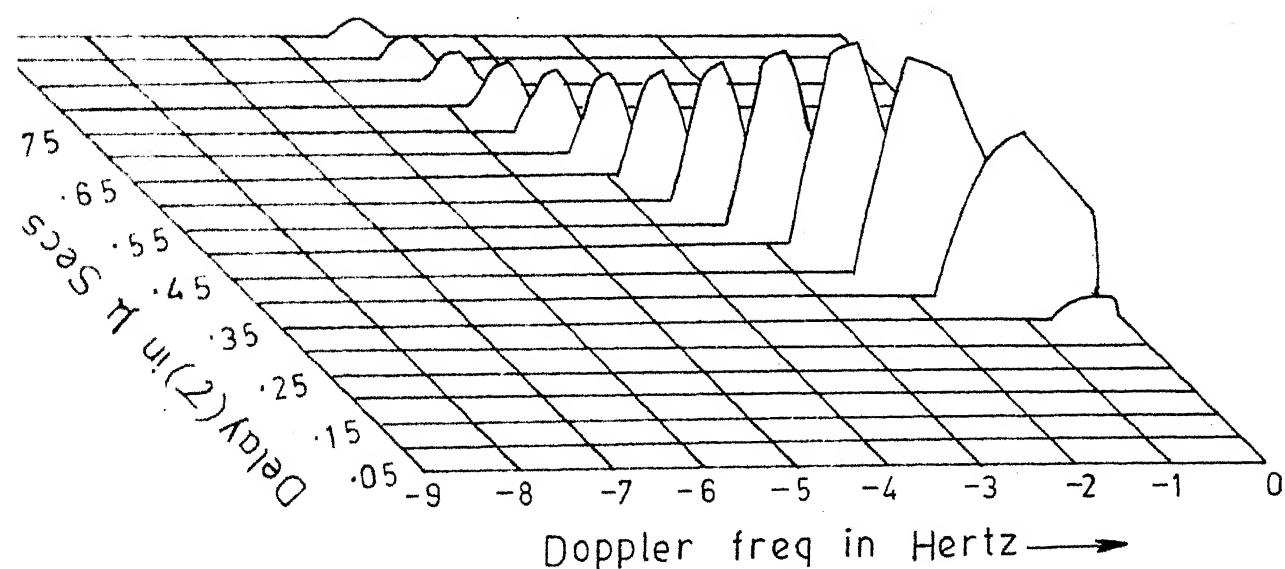
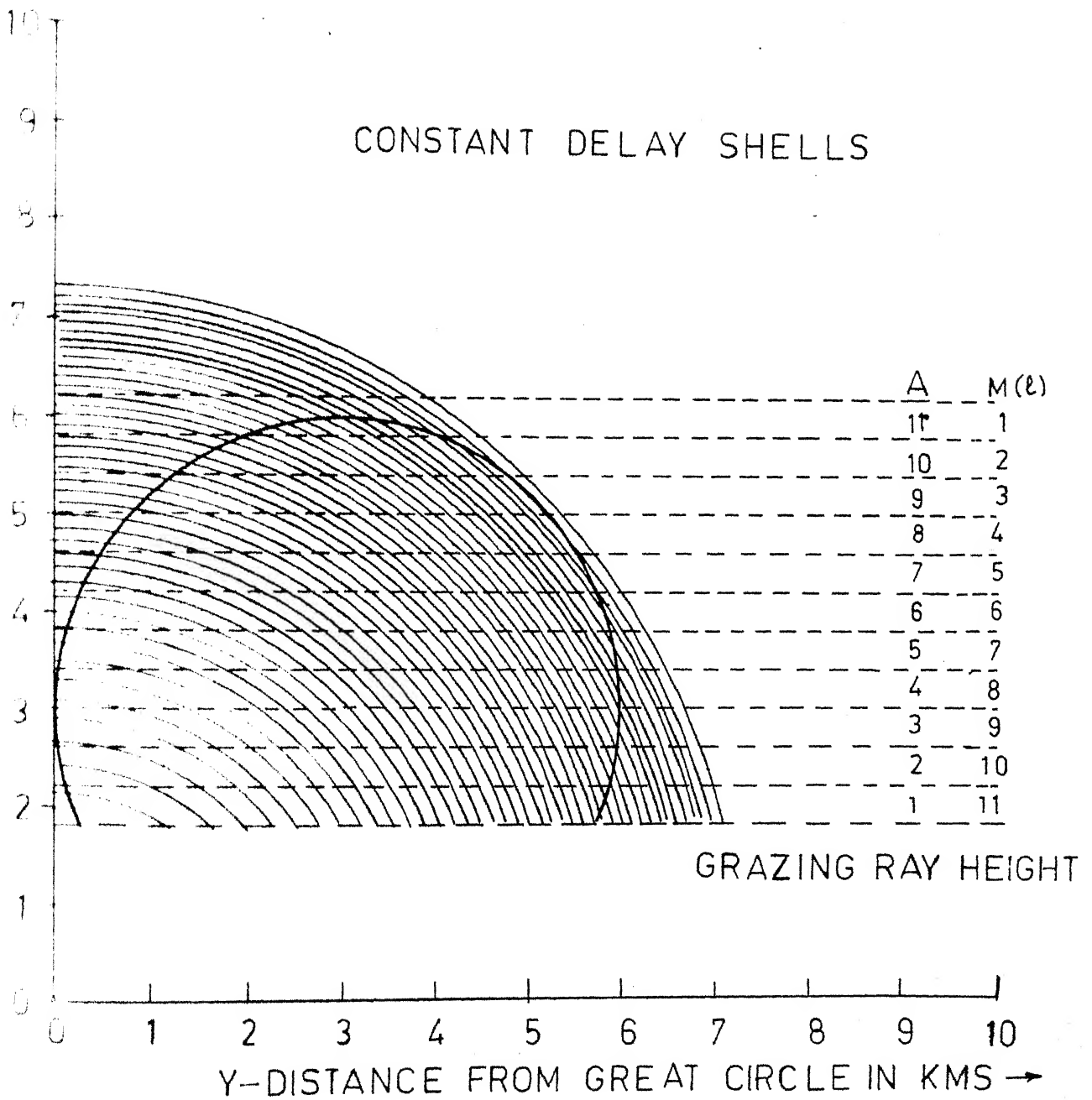


FIG.5-16

# CONSTANT DELAY SHELLS



### 5.2.6 Scattering functions : Set - 6

The scattering function results of this set correspond to multiple scattering layers in the common volume as shown in Fig. 5.18. Each layer shown in Fig. 5.18 has different degree of anisotropy ( $A$ ) and magnitude weighing function  $M(l)$ . The simulation program listings of Figs. 5.19 through 5.21 are given at Appendix (A-2). The important simulation parameters are given as under :

- a) Antenna azimuth off set ( $Y_c$ ) = 3 KMS
- b) Scattering layer heights, Anisotropy ( $A$ )  
weighting function ( $M(l)$ )

Layer No.	(KMS) Layer height	Anisotropy	$M(l)$
1.	1.8	1	11
2	2.2	2	10
3	2.6	3	9
4	3.0	4	8
5	3.4	5	7
6	3.8	6	6
7	4.2	7	5
8	4.6	8	4
9	5.0	9	3
10	5.4	10	2
11	5.8	11	1

# DELAY-DOPPLER POWER SPECTRUM: ANTENNA AZIMUTH OFFSET BY 3KMS FOR MULTILAYERS

$$Y_c = 3 \text{ KMS}$$

$$P = 2$$

$$\text{Scale: } \text{AMT} = 4.0 \times 10^{-4} \times \text{AMT}$$

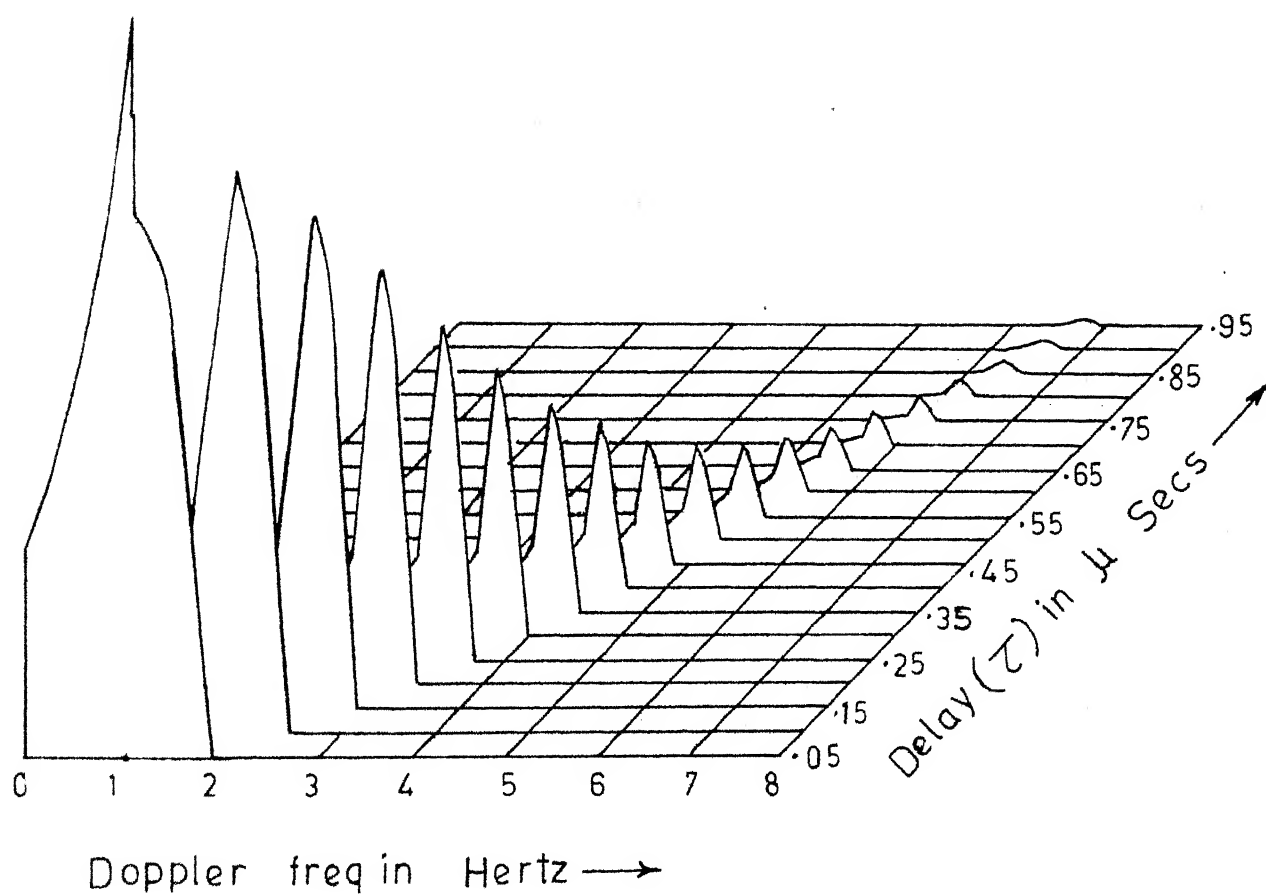


FIG. 5-19

# DELAY-DOPPLERPOWER SPECTRUM: ANTENNA AZIMUTH OFFSET BY 3KMS FOR MULTILAYERS

$$Y_c = 3 \text{ KMS}$$

$$P = 11/3$$

$$\text{Scale: } \text{AMT} = 4 \times 10^{-7} \times \text{AMT}$$

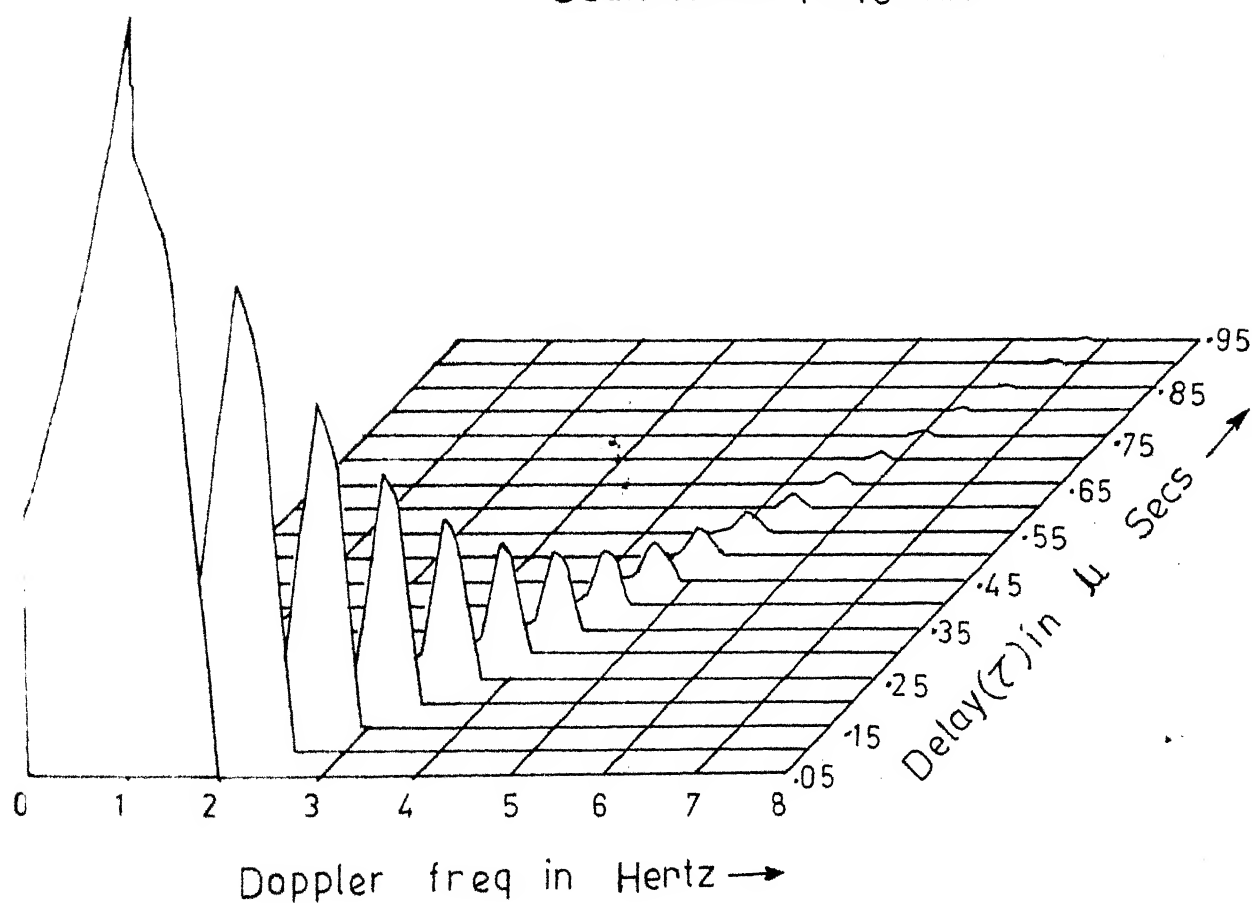


FIG.5-20



# DELAY DOPPLER POWER SPECTRUM: ANTENNA AZIMUTH OFFSET BY 3 KMS FOR MULTILAYERS

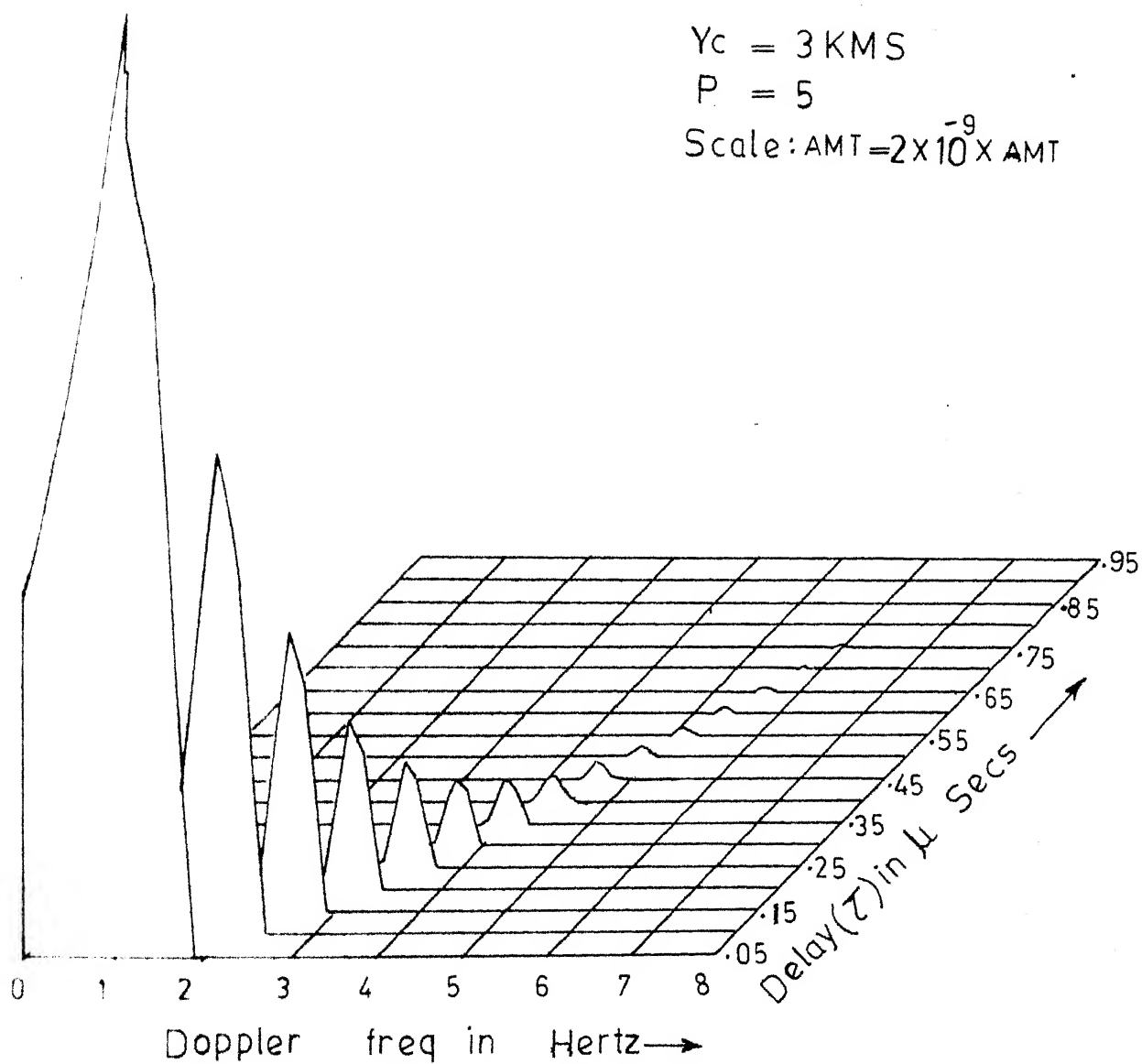


FIG. 5-21

- c) Thickness of each scattering layer = 400 Mtrs
- d)  $p = 2, \frac{11}{3}, 5$
- e) Gaussian circular antenna gain pattern of 3 KMS radius at mid path plane.

The resulting scattering functions are illustrated in Figs. 5.19 through 5.21. The observations given in Section 5.2.2 are valid. In addition the following are observed :

- a) The increase in power spectral density is due to the increase in scattering volume subtended by the time delay shells at the multiple scattering layers.
- b) The decrease in power spectral density for relative delays greater than 0.4 microsecs is due to the increase of anisotropy with height and decrease in scattering strength (magnitude weighting function  $M(l)$ ).

#### 5.2.7 Scattering functions : Set - 7

The simulation runs in this set are made to observe the effect of (i) degree of anisotropy (ii) the layer thickness on the power spectral density of scattering functions for the single scattering layer set up given in Section 5.2.2.

#### 5.2.7 (A) Run 1

The important simulation parameters are given as under :

- a) Antenna azimuth off set ( $Y_c$ ) = 3 KMS
- b) Single scattering layer at a height ( $SH_1$ ) = 3 KMS
- c) Scattering layer thickness = 400 Metrs
- d)  $p = \frac{11}{3}$
- e) Anisotropy ( $\Lambda$ ) = 10

The resulting scattering functions are illustrated in Fig.

5.22. The following observations are made :

- a) Zero doppler power spikes are noticed at the relative multipath delays of 0.1 and 0.15 microsecs
- b) For relative multipath delays greater than 0.2 microsecs, the power spectral density is negligible due to the anisotropic angular dependence function as given by

$$\sigma(\theta) = \left[ \frac{D^2}{\Lambda^2 Y^2 + Z_0^2} \right] \frac{11}{6}$$

- c) The effect of anisotropy is distinct, when compared with Fig. 5.6 which is simulated for isotropic layer ( $\Lambda = 1$ ).

#### 5.2.7 (B) Run - 2

The same simulation parameters given as in Section 5.2.7(A) are used for this Run also with anisotropy ( $\Lambda$ ) = 20.

DELAY-DOPPLER POWER SPECTRUM:  
ANTENNA AZIMUTH OFFSET BY 3 KMS

$$Y_c = 3 \text{ KMS}$$

$$P = 11/3$$

$$SH_1 = 3 \text{ KMS}$$

$$SH_2 = 34 \text{ KMS}$$

$$A = 10$$

$$\text{Scale: } \text{AMT} = 10^{-4} \times \text{AMT}$$

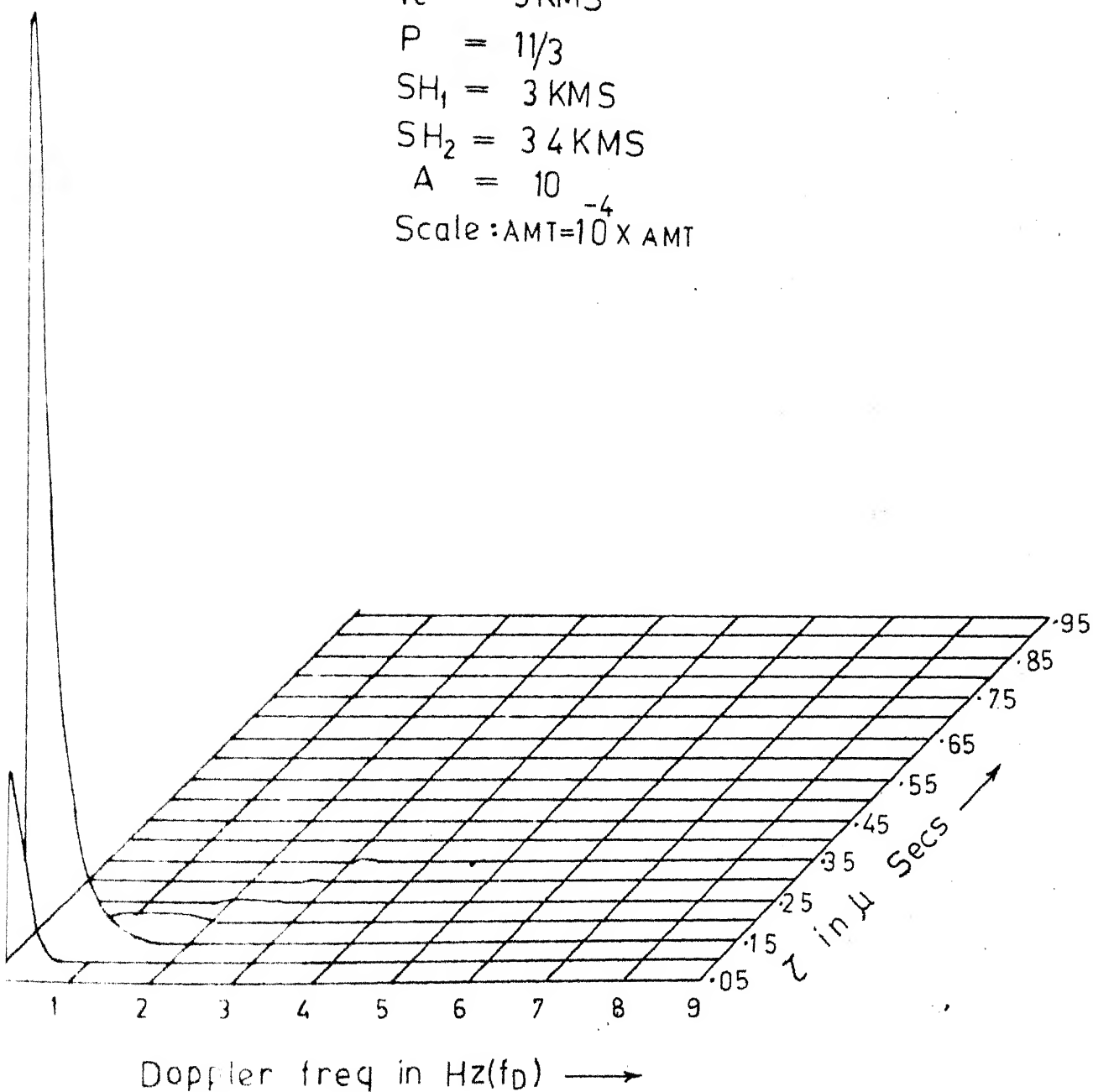


FIG.5-22

# FLAY-DOPPLER POWER SPECTRUM: ANTENNA AZIMUTH OFFSET BY 3 KMS

$$Y_c = 3 \text{ KMS}$$

$$P = 11/3$$

$$SH_1 = 3.0 \text{ KMS}$$

$$SH_2 = 3.4 \text{ KMS}$$

$$A = 20$$

$$\text{Scale: } MMT = 10^{-4} \times AMT$$

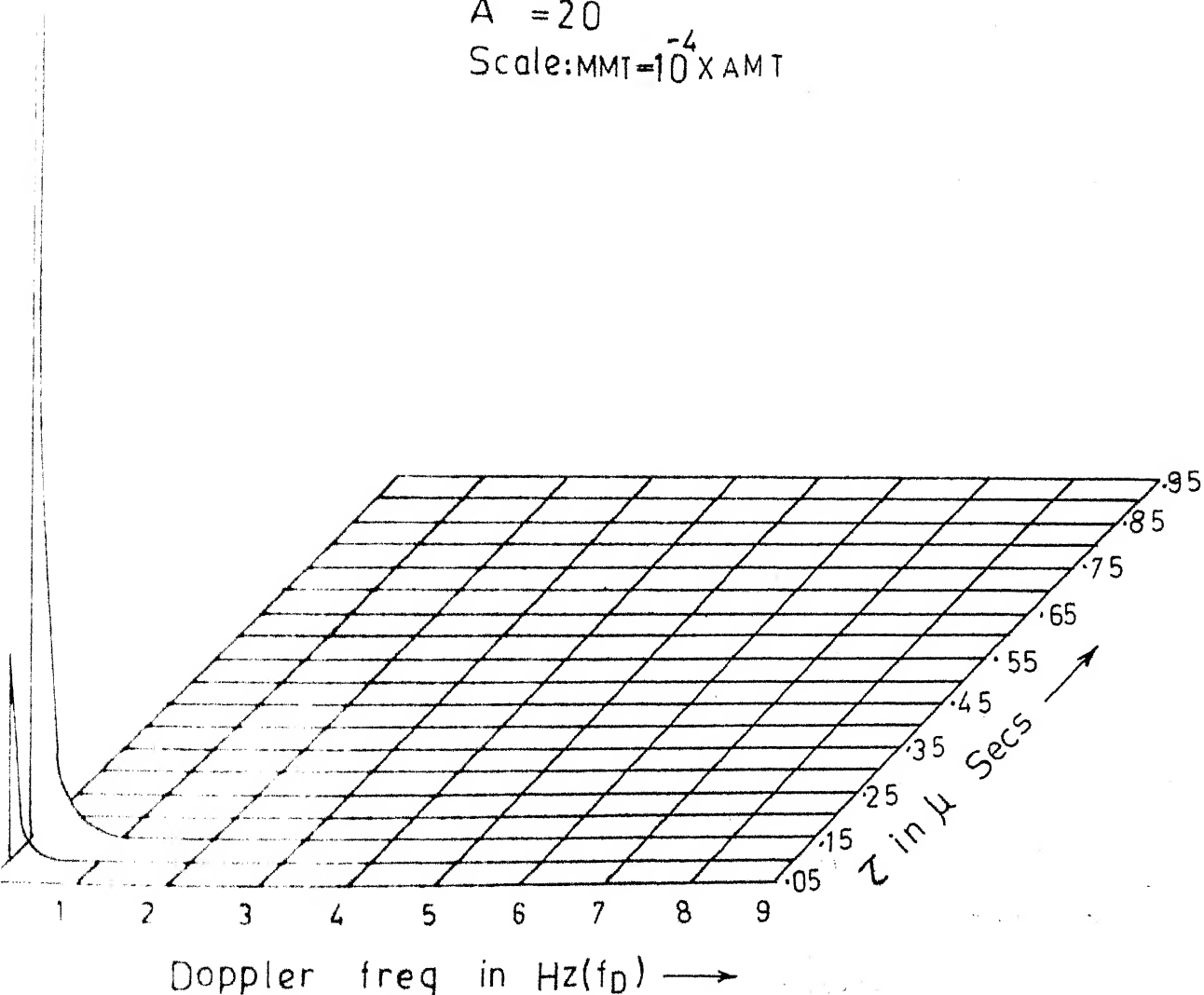


FIG.5-23

The resulting scattering functions are illustrated in Fig. 5.23. The observations given in Section 5.2.7(A) are valid for this run also.

#### 5.2.7 (C) Run - 3

The important simulation parameters are given as under :

- a) Antenna azimuth offset  $(Y_c) = 3$  KMS
- b) Single scattering layer at a height  $(SH_1) = 3$  KMS
- c) Scattering layer thickness = 800 Metres
- d)  $p = \frac{11}{5}$
- e)  $A = 1$

The resulting scattering functions are illustrated in Fig. 5.24. The observations given in Section 5.2.2 are valid. In addition the following are observed :

- a) When compared with scattering functions given in Fig. 5.6, the scattering functions obtained for this Run are flat due to small variation in scattering volume with cross path distance Y.

#### 5.2.7 (D) Run - 4

The same simulation parameters given as in Section 5.2.7(C) are used for this Run also with scattering layer thickness of 1200 Metres. The resulting scattering functions are illustrated in Fig. 5.25. The observations given in Section 5.2.7 (C) are valid for this run also.

# DELAY DOPPLER POWER SPECTRUM: ANTENNA AZIMUTH OFFSET BY 3KMS

$Y_c = 3 \text{ KMS}$   
 $P = 1\frac{1}{3}$   
 $SH_1 = 3 \text{ KMS}$   
 $SH_2 = 3.8 \text{ KMS}$   
 Scale:  $AMT = 10^{-5} \times AMT$   
 $A = 1$

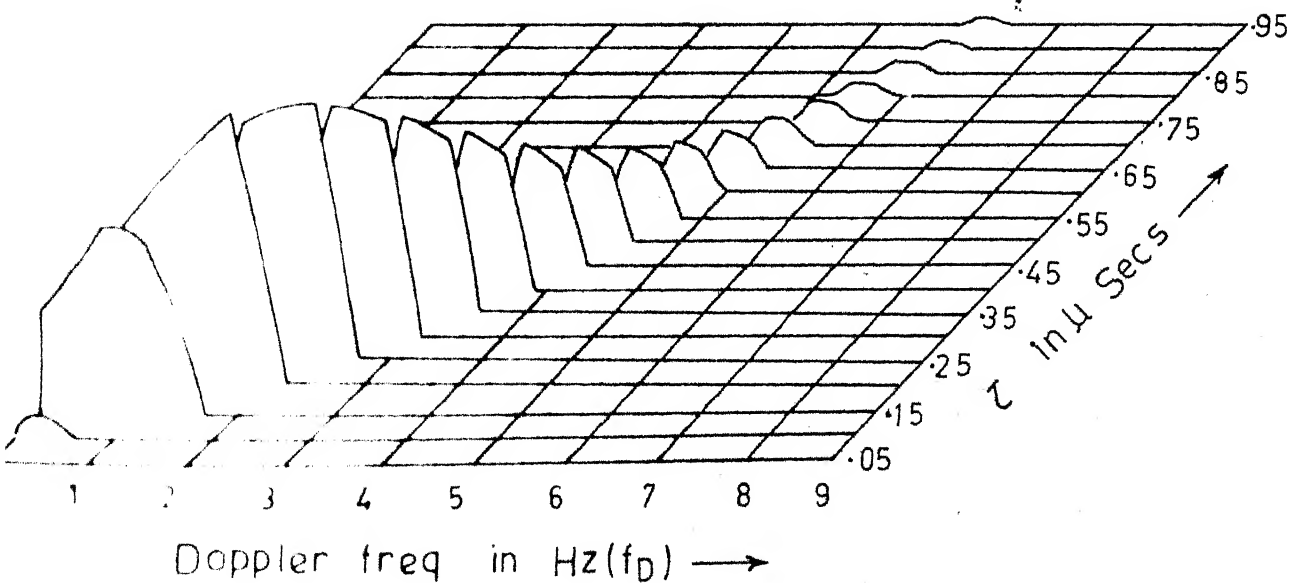


FIG. 5-24

# DELAY-DOPPLER POWER SPECTRUM: ANTENNA AZIMUTH OFFSET BY 3 KMS

$$Y_c = 3 \text{ KMS}$$

$$P = 11/3$$

$$SH_1 = 3 \text{ KMS}$$

$$SH_2 = 4.2 \text{ KMS}$$

$$\text{Scale: } \text{AMT} = 10^5 \times \text{AMT}$$

$$A = 1$$

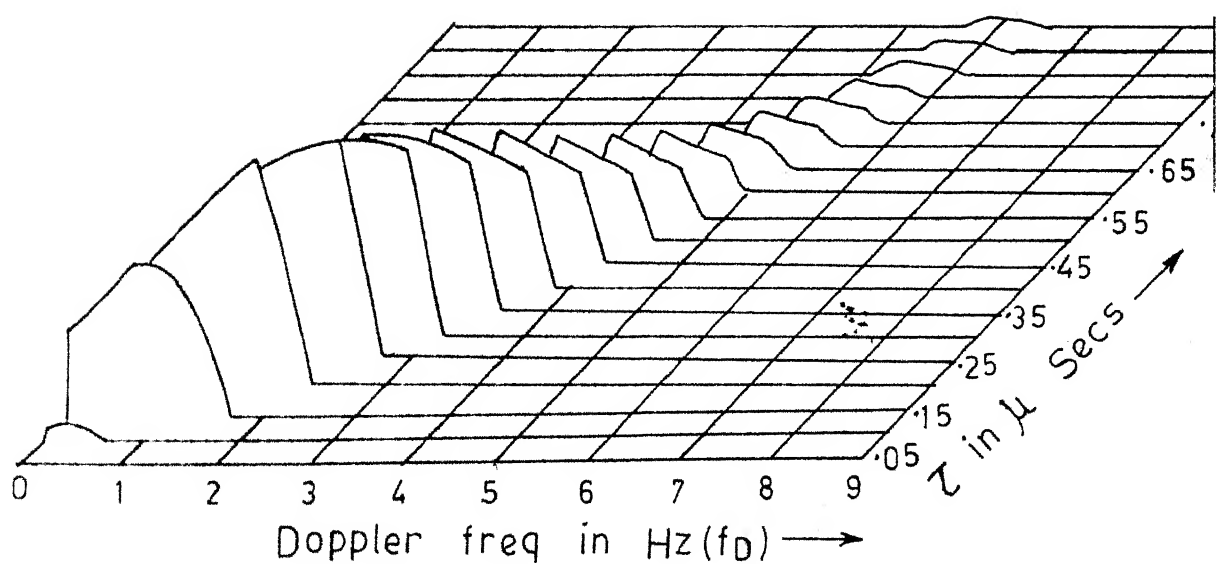


FIG. 5-25



## CHAPTER 6

6.1 Refractive Index Structure Function Coefficient  $C_n^2$ 

The structure function has been used by Tatarski [7] to describe the state of atmospheric turbulence. For fluctuations in the refractive index the structure function can be written

$$D_n(r) = C_n^2 r^{2/3} \quad L_0 \gg r \gg \ell_0 \quad (6.1)$$

$$\text{where } C_n^2 = a^2 L_0^{4/3} \left( \frac{d\bar{n}}{dz} \right)^2, \text{ called the} \quad (6.2)$$

structure function coefficient

$$a^2 = \text{a number close to 0.25 for sustained turbulence}$$

$$L_0 = \text{Outer scale of the isotropic turbulence in the inertial subrange (ranges from 10 to 100 Mtrs)}$$

$$\ell_0 = \text{inner scale of turbulence (order of millimeters)}$$

$$\frac{d\bar{n}}{dz} = \text{the average vertical gradient of refractivity}$$

Tatarski [7] has shown that when the radar's effective wavelength matches the eddy scales falling in the inertial subrange, then, the radar cross section of the isotropic refractive eddies is given by equation (4.14) and for  $p = \frac{11}{3}$ , we have

$$\sigma = 0.39 \times 2^{-11/3} C_n^2 \lambda^{-1/3} \sin^{-11/3} (\Theta/2) \quad (6.3)$$

where  $\lambda$  = the transmitted signal wavelength

$\Theta$  = the scattering angle

From (6.4), it is evident that for a troposcatter link having certain  $\lambda$  and  $\Theta$ , the power received is a measure of  $C_n^2$ .

Radiosonde measured  $C_n^2$  is a complicated function of pressure (P), temperature (T), mixing ratio (q), potential temperature gradient ( $\frac{d\theta}{dz}$ ) and potential mixing ratio gradient ( $\frac{dq}{dz}$ ).

From equation (6.2)  $C_n^2$  can be evaluated from radiosonde data by taking the outer scale  $L_0$  to be the nominal value of 100 meters and  $a^2 = 0.25$ .

## 6.2 Evaluation of $C_n^2$ from Rake Data

The power of the received signal, scattered at height Z, is given by the radar equation,

$$P_r = \frac{P_t G_t}{4\pi R^2} \frac{G_r}{4\pi R^2} \frac{\lambda^2}{4\pi} V \sigma(Z) \psi \quad (6.4)$$

where  $P_r$  = received power in Watts

$P_t$  = Transmitted power in Watts

$G_t, G_r$  = Transmitting and receiving antenna gains

- $V$  = Scattering volume in meters<sup>3</sup>  
 $R$  = Midpath distance in meters  
 $\lambda$  = Wavelength in meters  
 $\sigma(\theta)$  = Scattering cross section per unit volume in  
           meters<sup>-1</sup> as given in equation (6.3)  
 $\psi$  = Filling fraction of the common volume.

The equation (6.4) depends on the assumption that isotropic turbulence exists where  $C_n^2$  is measured. If not we can expect a discrepancy between the power received and the predicted by (6.4). This discrepancy is accounted by the assumption of anisotropy in the refractive structure.

For comparing the received signal intensity with the  $C_n^2$  parameter as a function of height, it is essential to determine the power per unit scattering volume as a function of height. For scattering layers, the power received at zero doppler shift observed in a particular Rake tape output is associated with the height of the tap's delay shell at the great circle plane. By substituting (6.3) in (6.4).

$$P_r = .39 P_t \frac{G_t G_r V \lambda^{5/3} 2^{-11/3} \psi \sin^{-11/3}(\theta/2) C_n^2}{4 \pi R^2 4 \pi R^2 4 \pi} \quad (6.5)$$

A numerical integration of the power density over that portion of the common volume that is seen by each correlator

is performed as given in [4] to find a satisfactory conversion of received power to  $C_n^2$ . The power density of the received signal due to single scattering from a point  $(X,Y,Z)$  is

$$\frac{dF_r}{dV} = \frac{-39 P_t G_t G_r \lambda^{5/3} C_n^2 2^{-11/3}}{(4\pi)^3} \left[ \frac{F_1(\Omega_1) F_2(\Omega_2)}{r_1^2 r_2^2} \sin^{-11/3}(\theta/2) \right] \quad (6.6)$$

where  $F_1(\Omega_1)$  = Transmitting antenna pattern at the point  $(X,Y,Z)$

$F_2(\Omega_2)$  = Receiving antenna pattern at the point  $(X,Y,Z)$

$R_1$  = Distance from transmitting antenna to the point at  $(X,Y,Z)$

$R_2$  = Distance from receiving antenna to the point at  $(X,Y,Z)$

Since only the zero doppler power is used to estimate  $C_n^2$  the evaluation of (6.6) is done for a point on  $(X,Z)$  plane for which  $Y = 0$

$\Omega_1 = \frac{Z}{D+X} - \phi_1 ; \phi_1$  = transmitting antenna elevation angle

$\Omega_2 = \frac{Z}{D-X} - \phi_2 ; \phi_2$  = receiving antenna elevation angle

$$R_1^2 = z^2 + (D + X)^2$$

$$R_2^2 = z^2 + (D - X)^2$$

$$\frac{D}{z} = \left( \frac{z}{D+X} + \frac{z}{D-X} \right) / 2$$

The relative power density from a scattering at a fixed height is obtained by considering only the factor

$$\left[ \frac{F_1(\alpha_1) F_2(\alpha_2)}{R_1^2 R_2^2} \sin^{-11/3} (\theta/2) \right]$$

and integrating this factor from  $-X_i$  to  $X_i$ , where  $X_i$  is the along path distance from the origin of the common volume corresponding to the  $i$ th correlator.

$$P_i(z) = \int_{-X_i}^{X_i} \frac{F_1(\alpha_1) F_2(\alpha_2)}{R_1^2 R_2^2} \sin^{-\frac{11}{3}} (\theta/2) dx \quad (6.7)$$

To find the relative total received power for each correlator it is necessary to integrate (6.7) over the vertical distance seen by each correlator. It is also necessary to include in this integration, the correlators gain function  $W(z)$ . Hence the relative zero doppler power from a correlator is given by

$$P_i(0) = \int_{Z_1}^{Z_2} W(z) P_i(z) dz \quad (6.8)$$

where  $(Z_2 - Z_1)$  = thickness of the chosen Rake tap delay shell.

A computer program is developed as per listings given in Appendix (A-3) for computing the relative zero doppler power received at each correlator. In this program, transmitting antenna gain pattern  $F_1(\theta_1)$  on (X,Z) plane is assumed to be Gaussian circular given by

$$F_1(\theta_1) = e^{-\frac{(Z - Z_c)^2}{Z_m^2}} \quad (6.9)$$

where  $Z_c$  = the height of the bore sight at the midpath plane from Transmitter - Receiver Chord line

$Z_m^2$  = Variance of the Gaussian pattern which is 2.6 KMS<sup>2</sup> for Kanpur - Nainital troposcatter link.

We have identical antennas at transmitter and Receiver. So,  $F_2(\theta_2)$  is given by

$$F_2(\theta_2) = e^{-\frac{(Z - Z_c)^2}{Z_m^2}} \quad (6.10)$$

So, the equation (6.7) becomes

$$P_1(Z) = \int_{-X_1}^{X_1} \frac{e^{-\frac{2(Z-Z_c)^2}{Z_m^2}} x^{\sin^{-1}11/3} (\theta/2)}{[Z^2 + (D+X)^2] [Z^2 + (D-X)^2]} dx$$

where  $\theta = 38.8$  MR } For Kanpur - Nainital troposcatter  
 $D = 165$  KMS } link.

A triangular correlator gain function is assumed in this program. The computed relative zero doppler power of the correlators is normalized by the maximum value which was found to be in the second correlator, set at the relative multipath delay of 0.10 microsecs. The results are tabulated in Table 1.

TABLE 1

<u>Correlator</u>	<u>Relative Power in dbs</u>
0.05	-2.68957
0.10	0
0.15	-0.45323
0.20	-1.04342
0.24	-2.48470
0.29	-4.33435

The table indicates that with a common volume uniformly filled with scatterers the observed relative zero doppler power from correlator one would be 2.68957 dB less than that from correlator two to convert it to a relative measure of  $C_n^2$ .

By knowing the power received in each correlator we can calculate the value of  $C_n^2$ .

For the existing troposcatter link between Kanpur - Mainital (CW signal) the long term median of the received power is -79 dBm. From this we can have rough estimate of the  $C_n^2$  value from the equation (6.4) given by

$$P_r = 10^{-10.9} \text{ Watts (for -79 dBm median)}$$

$$P_t = 1000 \text{ Watts}$$

$$G_t = G_r = 10^{4.5} \text{ (for } G_t = G_r = 45 \text{ db gain)}$$

$$V = 5.3 \times 10^9 \text{ metres}^3$$

$$\lambda = \frac{1}{7} \text{ metres}$$

$$R = 165 \times 10^3 \text{ metres}$$

Substituting the above values in equation (6.4), we can find out the value of  $\sigma(Z)$  as

$$\sigma(Z) = 1.3750 \times 10^{-6.9}$$

From equation (6.3) for Tatarski's model

$$\begin{aligned} \sigma(Z) &= 0.39 \times 2^{-11/3} C_n^2 \lambda^{-1/3} \sin^{-11/3}(\theta/2) = 1.3750 \times 10^{-6.9} \\ \therefore C_n^2 &= \frac{1.3750 \times 10^{-6.9} \times \lambda^{1/3} \times (\theta/2)^{11/3} \times 2^{11/3}}{.39} \\ &= 1.47 \times 10^{-12} \text{ metres}^{-2/3} \end{aligned}$$



Values of  $C_n^2$  in the range of  $10^{-13}$  to  $10^{-14}$  around a height of 1 KM appear to be consistent over the Indian Subcontinent as per the studies carried out by Mazumdar [8].

## CHAPTER 7

## CONCLUSION

7.1 Applications of the Simulated Scattering Functions

(a) From the scattering Functions obtained in Figs. 5.1 through 5.25, it is possible to obtain a reasonable estimate of the average cross path wind speed, layer altitudes and layer thicknesses. Equation (5.4) gives the delay - doppler locus for a layer given by

$$\tau = 2.8 \frac{\bar{f}_D^2}{\bar{V}^2} + \frac{\bar{Z}^2}{49.5} - .0655 \quad (7.1)$$

where  $\bar{f}_D$  = Average doppler shift for delay  $\tau$

$\bar{V}$  = Average cross path wind velocity

$\bar{Z}$  = Average scatter height

From Fig. 5.6, for the relative multipath delays of 0.2  $\mu$ secs and 0.55  $\mu$ secs, the average doppler shifts observed from the scattering functions are 1.5 Hz and 4.6 Hz respectively. Substituting the values of  $\tau$  and  $\bar{f}_D$  in (7.1), we obtain the following two equations, which we can solve for  $\bar{V}$  and  $\bar{Z}$ .

$$0.2655 = \frac{6.3}{\bar{V}^2} + \frac{\bar{Z}^2}{49.5}$$

$$\text{and, } 0.6155 = \frac{59}{V^2} + \frac{Z^2}{49.5}$$

$$\therefore \bar{V} = 12.2 \text{ Metres/sec}$$

$$\text{and, } \bar{Z} = 3.3 \text{ KMS}$$

The simulated values of  $\bar{V}$  and  $\bar{Z}$  are 11.8 metres/sec and 3.2 KMS respectively. So we notice the estimated values are very close to the simulated values.

From Fig. 5.6, it is observed that only two correlators having relative multipath delays 0.1 and 0.15  $\mu$ secs have zero doppler power. From equation (7.1) at great circle plane ( $\bar{f}_D = 0$ ), we can obtain the heights  $Z_2$  and  $Z_1$  corresponding to the delays 0.15 and 0.1  $\mu$ secs. By solving for  $Z_2$  and  $Z_1$  in equation (7.1), we have

$$Z_2 = 3.268 \text{ KMS}$$

$$Z_1 = 2.863 \text{ KMS}$$

Therefore, the scattering layer thickness is given by  $(Z_2 - Z_1)$  which is calculated as 405 Metres. So, it is seen that the layer thickness estimated from the scattering functions is very close to the simulated value which is 400 Metres.

(b) We can find the degree of anisotropy of the scattering layers from scattering functions, by knowing the power received at the Rake receiver correlators. From Figs. 5.22 and 5.23, it is noticed that the tracks display the increased angular dependence by having zero doppler spikes. The angular dependence for anisotropic model is given by equation (4.17) i.e. is,

$$\sigma(\theta) \sim \left[ \frac{D^2 \quad P/2}{A^2 Y^2 + Z^2} \right]$$

Therefore, by knowing the scattering cross section  $\sigma(\theta)$  for each correlator, we can obtain the value of A as a function of height (Z). And it is observed by Birkemeier [4] that the anisotropy increases with height.

(c) A simulation study of the type carried out here enables one to study the effects of antenna radiation pattern and pointing angle on the scattering function. Figs. (5.1) through (5.25) illustrate the effect of changing antenna effects upon scattering functions. This technique offers a means of estimating the performance of communication equipment under various known conditions of atmospheric structure.

(d) Results of this simulation program can be employed in conjunction with experimental Rake system data to

provide increased knowledge of the changing meteorological conditions of the troposphere. Obtaining experimental data under changing meteorological conditions will be very difficult because we don't know when such conditions will occur. Therefore, simulation studies of these infrequent events will save us the burden of continuously collecting the data.

## 7.2 Suggestions

In this simulation program uniform scatterer distribution is used. However, various scatterer distributions such as Gaussian, poisson etc can be employed to determine which distribution most closely represent the physical situation. And the effects of various forms of scatterers can also be studied if equations that describe the reflection, refraction and absorption characteristics of the scatterers can be written.

## APPENDIX (A-1)

```

C      THIS PROGRAM SIMULATES THE CONSTANT DELAY SHELLS OF THE
C      EXPERIMENTAL
C      PROPOSCATTER LINK BETWEEN KANPUR AND NAINITAL. THE DELAY
C      SHELLS ARE
C      CONCENTRIC CIRCLES ON Y-Z PLANE WITH INCREMENTS OF 0.025  $\mu$ SE
C      THE ASSUMED GAUSSIAN CIRCULAR ANTENNA PATTERN AND AN
C      HYPOTHETICAL
C      SCATTERING LAYER IS SUPERPOSED ON THE DELAY SHELLS.
C      LINK PARAMETERS
C      C--VELOCITY OF LIGHT IN KMS/SEC
C      D--HALF THE DISTANCE BETWEEN TRANSMITTER AND RECEIVER IN KMS
C      YA AND ZA-- Y AND Z COORDINATES IN KMS OF THE CENTRE OF THE
C      CIRCLE OF THE
C      ANTENNA PATTERN. THESE COORDINATES KEEP CHANGING DEPENDING
C      UPON THE
C      AZIMUTHAL AND ELIVATION ANTENNA OFF SETS.
C      R-- THE RADIUS OF THE CIRCULAR ANTENNA PATTERN AT THE
C      MIDDLE IN KMS
C      SH1--HEIGHT OF THE SCATTERING LAYER IN KMS FROM THE
C      TRANSMITTER
C      RECEIVER CHORD LINE
C      SH2--SH1+THICKNESS OF THE SCATTERING LAYER IN KMS
C      ZG--GRAZING RAY HEIGHT IN KMS
C
C  // JOB
C  // FOR DLINE
C      THIS SUBROUTINE IS FOR DRAWING THE DOTTED LINES AT THE
C      HEIGHT ZG, SH1 AND
C      SH2 INDICATING GRAZING RAY HEIGHT AND SCATTERING LAYER
C      SUBROUTINE DLINE (Z,YINC)
C      Y=.0
C      CALL DPLOT(1,Y,Z)
C      1 Y=Y+YINC
C      CALL FPLOT(2,Y,Z)
C      Y=Y+YINC
C      CALL FPLOT(1,Y,Z)
C      IF(Y-13.)1,2,2
C      2 RETURN
C      END
C
C  // FOR MAIN
C      NONPROCESS PROGRAM
C      ONE WORD INTEGERS
C      IOCS(PLOTTER,CARD)

```

```

DATA C /3.E5/
DATA D,ZG / 165., 1.8 /
CALL SCALF(.6,.6,.0,.0)
C PLOTTER ROUTINES FOR DRAWING THE Y-Z GRID LINES-
CALL FGRID(1,.0,.0,1.,13)
CALL FGRID(0,.0,.0,1.,13)
READ(5,100)SH1,SH2
READ(5,100)YA,ZA,R
C PLOTTING THE DOTTED LINES STARTS HERE
CALL DLINE(ZG,.25)
CALL DLINE(SH1,.125)
CALL DLINE(SH2,.125)
C PLOTTING OF THE CIRCULAR ANTENNA PATTERN STARTS HERE
CSANG=(ZA-ZG)/R
ANGL=ATAN(SQRT(1.-CSANG **2)/CSANG)
AINC=(3.14159-ANGL)/100.
IPEN=-2
DO 30 I=1,201
Y=YA+R SIN(ANGL)
Z=ZA-R COS(ANGL)
CALL FPLLOT(IPEN,Y,Z)
IPEN=0
30 ANGL=ANGL+AINC
C NOMOGRAMS WRITING WITH THE HELP OF THE PLOTTER STARTS HERE
HT=(SH2-SH1)*.36
IF(HT-.15)31,31,32
31 CALL FCHAR(7.,SH1+(SH2-SH1)*.2,HT*.67,HT,.0)
GOTO 33
32 CALL FCHAR(7.,SH1+(SH2-SH1)*.5-.125,.1,.15,.0)
33 CONTINUE
WRITE(7,101)
101 FORMAT('SCATTERING LAYER')
CALL FCHAR(7.,1.35,.10,.15,.0)
WRITE(7,102)
102 FORMAT('GRAZING RAY HEIGHT')
Y=.15
DO 35 I=1,14
J=I-1
CALL FCHAR(-.6,Y,.10,.15,.0)
WRITE(7,105)J
105 FORMAT(12)
35 Y=Y+1.
X=-.3
DO 40 I=1,14
J=I-1
CALL FCHAR(X,-.5,.10,.15,.0)
WRITE(7,105)J

```

```

40  X=X+1.
    CALL FCHAR(7.0,-1,.10,.15,.0)
    WRITE(7, 103)
103  COMMENT('Y - DISTANCE FROM GREAT CIRCLE IN KM')
    CALL FCHAR(-.8,5.,.10,.15,1.5708)
    WRITE(7,104)
104  FORMAT('Z - HEIGHT ABOVE SURFACE IN KILOMETRES')
    CALL FCHAR(8.,12.,.12,.18,.0)
    WRITE(7,106)
106  FORMAT('CONSTANT DELAY SHELLS')
C    NOMOGRAMS WRITING ENDS HERE
C    TOUIV--RELATIVE DELAY CORRESPONDING TO THE FIRST DELAY SHELL
C    TOUIN--RELATIVE DELAY INCREMENTS FOR THE SUBSEQUENT
C    DELAY SHELLS
C    TOUFV--RELATIVE DELAY CORRESPONDING TO THE LAST DELAY SHELL
    READ(5,100)TOUIV,TOUIN,TOUFV
100  FORMAT(3F8.3)
    TOUFV=TOUFV+TOUIN*.5
C    INITIALISATION OF THE RELATIVE DELAY TOU
    TOU=TOUIV
C    INITIALISATION OF THE Z COORDINATE OF THE DELAY SHELL
10  Z=ZG
    DZG=SQRT(D*D+ZG*ZG)
    CT=(.5*C*TOU*1.E-6+DZG)**2-D*D)
C    PLOTTING OF THE FIRST DELAY SHELL STARTS HERE
    CALL FPLLOT(1,SQRT(CT-Z*Z),Z)
    ZINC=(SQRT(CT)-ZG)/200.
    IPEN=2
    DO 15 I=1,200
    Z=Z+ZINC
    CALL FPLLOT(IPEN,SQRT(CT-Z*Z),Z)
C    PLOTTING OF THE FIRST DELAY SHELL ENDS HERE
15  IPEN=0
C    RELATIVE DELAY FOR THE NEXT DELAY SHELL IS SET HERE
    TOU=TOU+TOUIN
    IF(TOU-TOUFV)10,10,99
99  STOP
    END
// XEQ MAIN
CCEND
3.0      3.4
3.0      3.0      3.0
0.0      .025      1.0

```



## APPENDIX (A-2)

```

C   THIS PROGRAM SIMULATES THE DELAY-DOPPLER POWER SPECTRA
C   OF THE
C   PROPOSED EXPERIMENTAL TROPOSCATTER LINK BETWEEN KANPUR AND
C   RAINITAL
C   USING RAKR SYSTEM-IT IS ASSUMED THAT THE SCATTERERS ARE
C   UNIFORMLY
C   DISTRIBUTED IN A DISCRETE SCATTERING LAYERS-GAUSSIAN
C   CIRCULAR ANTENNA
C   RADIATION PATTERN IS ASSUMED
C   LINK PARAMETERS
C   SH1--HEIGHT OF THE SCATTERING LAYER IN KMS FROM THE
C   TRANSMITTER-RECEIVER CHORD LINE
C   SH2--SH1+THICKNESS OF THE SCATTERING LAYER IN KMS
C   ZG--GAZING RAY HEIGHT IN KMS
C   D--HALF THE DISTANCE BETWEEN TRANSMITTER AND RECEIVER IN KMS
C   ZZERO--MEAN HEIGHT OF THE SCATTERERS IN KMS GIVEN BY
C   (SH1+SH2)*0.5
C   YC--ANTENNA AXI:UTH OFF SET IN KMS AT THE MIDPATH PLANE
C   YMSQ--ANTENNA PATTERN VARIANCE IN KMSQ ON,Y--AXIS.
C   YMSQ IS 2.6 KMSQ FOR THIS LINK
C   TOU--RELATIVE MULTIPATH DELAY IN MICROSECS AT WHICH THE
C   RAKE TAPS ARE SET- IN THIS WORK THE RAKE TAPS SARE SET
C   AT 0.05 MICROSECS APART
C   TOU1 AND TOU2--THE LOWER AND UPPER MULTIPATH DELAYS
C   CORRESPONDING TO EACH RAKE TAP
C   A--THE DEGREE OF ANISOTROPY ASSOCIATED WITH EACH LAYER
// JOB
// FOR CTR
IOCS(CARD,PLOTTER)
ONE WORD INTEGERS
NONPROCESS PROGRAM
  READ(5,100)SH1,SH2,ZG,A,D,ZZERO,YC,YMSQ,TOU1,TOU2
100  FORMAT(10F8.3)
C   SCLF--SCALE FOR DOPPLER FREQ IN INCHES PER HERTZ
C   SCLP--SCALE FOR THE AMPLITUDE OF THE POWER SPECTRAL DENSITY
C   HDISP AND VDISP--HORIZONTAL AND VERTICAL DISPLACEMENT OF
C   THE ORIGIN
C   PER INCREMENT IN MULTIPATH TIME DELAY(TOU) WITH RESPECT TO
C   THE ORIGIN OF THE INTIAL VALUE OF TOU
C   READ(5,101)SCLF,SCLP,HDISP,VDISP
101  FORMAT(4F8.2)
C   N1--TOTAL LENGTH OF TOU AXIS IN TERMS OF NO OF VDISP
C   INCI:MENTS
C   N2--NO OF INCLINED GRID LINES ON DOPPLER FREQ AXIS
C   DFRIV--DOPPLER FREQ INTIAL VALUE FOR DRAWING INCLINED GRID
C   LINES
C   DFRIN--DOPPLER FREQ INCRIMENTS IN HERTZ
C   READ(5,102)N1,N2,DFRIV,DFRIN

```

```

102  FORMAT (2I4,2F8.1)
      CALL SCALF(SCLF,SCLP,DFRIV,.0)
      HDISP=HDISP/SCLF
      VDISP=VDISP/SCLP
      TVDSP=VDISP*N1
      THDSP=HDISP*N1
      B=DFRIV
C    DRAWING OF INCLINED GRID LINES STARTS HERE
      DO 10 I=1,N2
      CALL FPLOT(-2,B,.0)
      CALL FPLOT(-1,B+THDSP,TVDSP)
C    DRAWING OF INCLINED GRID LINES ENDS HERE
10   B=B+DFRIN
C    INITIALISTTION OF HORIZONTAL AND VERTICAL DISPLACEMENTS
C    CORRESPONDING TO INTIAL TOU
      HDISP=0.0
      VDISP=0.0
      CALL FPLOT(1,DFRIV,.0)
      DZG=SQRT(D*D+ZG*ZG)
C    R1 AND R2--INNER AND OUTER RADII OF THE CONSTANT DELAY
      SHELL CORRESPONDING
C    TO TOU1 AND TOU2 RESPECTIVELY
      R1=SQRT((0.15*TOU1+DZG)**2-D*D)
7    R2=SQRT((0.15*TOU2+DZG)**2-D*D)
      TOU=TOU2-0.025
C    Y AND YT--ARE THE ACTUAL AND PLOTTER FREQ CO-ORDINATES
      Y=0.0
      YT=HDISP
      CALL FPLOT(1,YT,VDISP)
C    BRANCHING OUT FOR DIFFERENT CASES FOR THE PURPOSE OF
      COMPUTING THE
C    AREA SUBTENDED BY THE CHOOSEN DELAY SHELL AND THE SCATTERIN
      LAYER
      IF(R2-SH1)4,4,71
71   IF(R2-SH2)12,12,82
82   IF(R1-SH1)22,22,72
72   IF(R1-SH2)23,23,73
C    DFRSV--DOPPLER SHIFT STARTING VALUE CORRESPONDING TO THE
C    INTERSECTION POINT OF THE RADIUS R1 AND THE
C    SCATTERING LAYER HEIGHT SH2
C    DFRS1-POINT ON THE DOPPLER SHIFT AXIS CORRESPONDING TO THE
C    INTERSECTION OF THE RADIUS R1 AND THE SCATTERING LAYER
      HEIGHT SH1
C    DFRS2--POINT ON THE DOPPLER SHIFT AXIS CORRESPONDING TO THE
      INTERSECTION
C    OF THE RADIUS R2 AND THE SCATTERING LAYER HEIGHT SH2

```

```

C   DFREV--DOPPLER SHIFT END VALUE,CORRESPONDING TO THE
      INTERSECTION OF
C   RADIUS R2 AND THE SCATTERING LAYER HEIGHT SHL
73  DFRSV=SQRT(R1*R1-SH2*SH2)
C   FOR THE PURPOSE OF COMPUTATION OF THE AMPLITUDE OF THE
      POWER SPECTRAL
C   DENSITY DOPPLER SHIFT FREQ AXIS IS DEVIDED IN TO STEPS
      0.02 HERTZ
      N=DFRSV/0.02
      Y=FLOAT(N) 0.02+0.02
      YT=Y+HDISP
      CALL FPLOTT(2,YT,VDISP)
23  DFRSI=SQ RT(R1*R1-SH1*SH1)
22  DFREV=SQRT (R2*R2-SH1*SH1)
      DFRS2=SQRT(R2*R2-SH2*SH2)
C   BRANCHING OUT FOR THE DIFFERENT CASES FOR COMPUTATION OF
      THE COMMON VOLUME
C   AREA CORRESPONDING TO EACH CORRELATOR TIME DELAY
      6 IF(Y-DFRS1)1,74,74
74  IF(Y-DFRS2)2,75,75
75  IF(Y-DFREV)76,76,4
76  AREA=SQRT(R2*R2-Y*Y)-SH1
      GO TO 5
      1 IF(Y-DFRS2)77,77,3
77  AREA=SH2-SQRT(R1*R1-Y*Y)
      GOTO 5
      2 AREA=SH2-SH1
      GOTO 5
      3 AREA=SQRT(R2*R2-Y*Y)-SQRT(R1*R1*Y*Y)
      5 CALL AMP(AREA,D,A,Y,ZZERO,YC,YMSQ,VDISP,YT,HDISP)
      YT=Y+HDISP
      GOTO 6
12  DFREV=SQRT(R2*R2-SH1*SH1)
      IF(R1-SH1)19,19,14
19  IF(Y-DFREV)78,78,4
78  AREA=SQRT(R2*R2-Y*Y)-SH1
      CALL AMP(AREA,D,A,Y,ZZERO,YC,YMSQ,VDISP,YT,HDISP)
      YT=Y+HDISP
      GOTO 19
14  DFRS1=SQRT(R1*R1-SH1 SH1)
21  IF( Y-DFRS1)15,89,89
89  IF(Y-DFREV)79,4,4
79  AREA=SQRT(R2*R2-Y*Y)-SH1
      GOTO 18

```

```

15 AREA=SQRT(R2*R2-Y*Y)-SQRT(R1*R1-Y*Y)
18 CALL AMP(AREA,D,A,Y,ZZERO,YC,YMSQ,VDISP,YT,HDISP)
   YT=Y+HDISP
   GOTO 21
C   COMPUTATION FOR PRESENT TOU ENDS
   4 R1=R2
     CALL FPLLOT(2,9.0+HDISP,VDISP)
     TOU2=TOU2+0.05
     HDISP=HDISP+0.25
     VDISP=VDISP+0.25
     IF(TOU2-1.0)7,7,80
   80 CALL EXIT
     END
C   SUBROUTINE FOR COMPUTING THE AMPLITUDE OF THE POWER
C   SPECTRAL DENSITY
// FOR CALC
   SUBROUTINE AMP(AREA,D,A,Y,ZZERO,YC,YMSQ,VDISP,YT,HDISP)
   ANTC=EXP(-(YC-Y)**2/(YMSQ))
   SCATC=(D*D/(A*A*Y*Y+ZZERO*ZZERO))**1.8333333
   AMT=SCATC*AREA*ANTC*1.0E-5+VDISP
   CALL FPLLOT(0,YT,AMT)
   Y=Y+0.02
   RETURN
   END
// KEQ CTR
*CCEND

```

## APPENDIX (A-3)

```

C      THIS PROGRAM SIMULATES THE RELATIVE ZERO DOPPLER
C      POWER OF CORRELATORS. THIS GIVES THE RELATIVE MEASURE
C      OF CN SQUIRE
// JOB
// FOR CTR
IOCS(CARD,TYPEWRITER)
ONE WORD INTEGERS
NONPROCESS PROGRAM
C      THETA--SCATTERING ANGLE IN RADIANTS, GAMA-3DB ANTENNA
C      BEAM-WIDTH IN RADIANTS,
C      TOULANDTOU2 CORRESPOND TO FIRST CORRELATOR TIME DELAY
D      SHELL IN MICROSECS
      READ(5,101) THETA,GAMA,TOUL,TOU2
101    FORMAT(4F8.4)
C      D-TRANSMITTER-RECEIVER MIDPATH DISTANCE IN KMS,ZG--
C      GRAZING RAY HEIGHT IN
C      KMS,ZMSQ-VARIANCE OF ANTENNA PATTERN IN KMS
      READ(5,102)D,ZG,ZMSQ
102    FORMAT(3F8.3)
C      THE FACTOR(SIN(THETA/2))**-11/3 IS COMMON FOR ALL COMPUTA
C      AND ANGF IS
C      THE SMALL ANGLE ANGLE APPROXIMATION OF THE ABOVE FACTOR
      ANGF=(THETA*0.5)**(-3.667)
C      ZC-HEIGHT OF THE MIDPOINT OF THE COMMON VOLUME FROM
C      TRANSMITTER-RECEIVER
C      CHORD
      ZC=D*THETA*0.5
      DZG=SQRT(D*D+ZG*ZG)
C      Z1AND Z2 ARE THE HEIGHTS WHERE THE DELAY SHELLS OF EACH
C      CORRELATOR
C      CUT THE Z-AXIS).AND THUS(Z2-Z1) IS THE COMMON VOLUME
C      THICKNESS OF THE
C      CORRELATOR
      Z1=SQRT((0.15*TOUL+DZG)**2-D*D)
31    Z2=SQRT((0.15*TOU2+DZG)**2-D*D)
C      ZINC IS THE INCRIMENTAL STEP OF THICKNESS (Z2-Z1)
C      CORRESPONDING TO
C      EACH CORRELATOR FOR EVALUATING THE OUTER INTEGRAL
      ZINC=(Z2-Z1)*0.05
C      TOU-RELATIVE MULTIPATH DELAY OF THE CORRELATOR
      TOU=TOU2-0.025
C      ZMEAN IS THE MEAN VALUE OF Z1AND Z2 USED FOR THE PURPOSE
C      OF COMPUTING

```

```

C      THE LENGTH ON POSITIVE AXIS OF THE COMMON VOLUME
C      CORRESPONDING TO EACH
C      CORRELATOR DENOTED BY XE. LENGTH EXTENDS FROM -XE TO XE
      ZMEAN=(Z1+Z2)*0.5
C      DIFFERENT FORMULAE ARE APPLICABLE FOR COMPUTING XE
C      FOR ZMEAN ABOVE
C      AND BELOW ZC.
      IF(ZMEAN-ZC)21,21,22
21     XE=(2.0 ZMEAN)/(THETA-GAMA)-D
      GOTO 23
22     XE=D-(2.0 ZMEAN)/(THETA+GAMA)
C      XINC IS THE INCREMENTAL STEP OF COMMON VOLUME LENGTH
C      FOR EVALUATING
C      THE INNER INTEGRAL
23     XINC=XE*0.05
C      INITIALISATION OF THE OUTER INTEGRAL
      Z I=0.0
C      INITIALISATION OF Z TAKEN TO BE THE MID POINT OF THE FIRST
C      INCREMENTAL STEP
      Z=Z1+0.5*XINC
C      COMPUTATION OF THE OUTER INTEGRAL STARTS
      DO 30 I=1,20
      S=I
C      F=F1*F2, WHERE , F1=F2 ARE THE GAUSSIAN CIRCULAR ANTENNA
C      PATTERNS ABOUT Z AXIS
      F=EXP(-2.0*(Z-ZC)**2/ZMSQ)
C      COMPUTATION OF THE CORRELATOR GAIN FACTOR, WZ, WHICH VARIES
C      ZERO TO ONE FOR THE FIRST HALF OF THE CORRELATOR THICKNESS
C      AND FROM
C      ONE TO ZERO FOR THE LATTER HALF
      IF(I-10)24,24,25
24     WZ=S*0.1-0.05
      GOTO 26
25     WZ=2.0-S*0.1+0.05
C      INITIALISATION OF THE INNER INTEGRAL
26     XI=0.0
C      INITIALISATION OF THE X VALUE, TAKEN TO BE THE MID POINT
C      OF THE FIRST INCREMENTAL STEP
      X=-XE+0.5*XINC
C      COMPUTATION OF THE INNER INTEGRAL STARTS
      DO 40 J=1,40
C      R1SQ AND R2SQ ARE THE SQUARES OF THE DISTANCES OF THE
C      SCATTERING POINT
C      FROM THE RECEIVING ANTENNA AND TRANSMITTING ANTENNA
C      RESPECTIVELY

```

```

RISQ=Z *Z+(D+X) **2
R2SQ=Z *Z+(D-X) **2
XI=XI+1.0/(R1SQ *R2 SQ)
40 X=X+XINC
C   COMPUTATION OF THE INNER INTEGRAL STARTS
    ZI=ZI+XI *WZ *F
30 Z=Z+ZINC
C   COMPUTATION OF THE OUTER INTEGRAL ENDS
C   ZDP--RELATIVE ZERO DOPPLER POWER OF EACH CORRELATOR IN I
    ZDP=10.0 *ALOG(ZI *ANGF)/2.3
    WRITE(1,100)TOU,ZDP
100 FORMAT(/10X,F5.2,10X,F8.5)
C   FOR COMPUTING ZDP OF THE NEXT CORRELATOR
    Z1=Z2
    TOU2=TOU2+0.05
C   AS THE VALUE OF Z2 CORRESPONDING TO TOU2 GREATER THAN
C   0.325 FALLS
C   OUTSIDE THE COMMON VOLUME THE COMPUTATION ENDS
    IF(TOU2-0.35)31,31,32
32 CALL EXIT
    END
//XEQ CTR
CCEND
    0.0388    0.0166    0.025    0.075
165.0        1.8        2.6

```

## REFERENCES

- [1] Price, R. and Green, P.E., 'A communication Technique for multipath channels', Proc. IRE Vol. 46, pp 555-570, Mar 1958.
- [2] Barrow, B.B., Abraham, L.G., COWAN, W.M., Gallant, R.M., 'Indirect Atmospheric measurements utilizing Rake Tropospheric scatter Techniques - Part I : The Rake Tropospheric Scatter Technique', Proc. IEEE, Vol. 57, No.4, pp 537-551, April 1969.
- [3] Birkemeier, W.P., Merrill, H.S., Sargeant, D.H., Thomson, D.W., 'Indirect Atmospheric Measurements Utilizing Rake Tropospheric Scatter techniques - Part II: Radiometeorological Interpretations of Rake channel - Sounding Observations', Proc. IEEE, Vol. 57, No.4, pp 552-559, April 1969.
- [4] Birkemeier, W.P., Fontaine, A.B., Gage, K.S., Jasperson, W.H., 'A comparison of Rake - Measured Scattering Layer Signatures with Radiosonde Data', RADC-TR-74-17, Rome Air Development Center, Final Technical Report, Feb 1974.
- [5] Gupta, G.C., 'Tropospheric probing by scatter communication', M.Tech. Thesis (1973), I.I.T. Kanpur.



- [6] Pool, R.H., 'The Development and Application of a Digital Computer Simulation of the Rake concept as related to Tropospheric Scatter Measurement', Ph.D. Thesis, The University of IOWA, Electrical Engineering, 1972.
- [7] Tatarski, V.I., 'Wave propagation in a Turbulent Medium,' McGraw-Hill, New York, 1961.
- [8] Majumdar, S.C., 'Transhorizon Tropospheric Propagation Studies Over the Indian Subcontinent', Centre of Research on Troposphere, National Physical Laboratory, Report No. 13, March 1974.